Peretti Museum Foundation

Journal of Applied Ethical Mining of Natural Resources and Paleontology 2, 1-35 (2021).

Peretti A. [1, 2] **and Bieri W.** [1]**:** PMF data depository of analysis FTIR-ATR, PL analysis, CT scan and UV imaging of amber containing holotype Yaksha perettii, Oculudentavis naga and comparative amber samples, and associated invertebrate inclusions.

[1] *GRS Gemresearch Swisslab AG Baumschulweg 13 6045 Meggen, Switzerland*

[2] *Peretti Museum Foundation, Baumschulweg 13, 6045 Meggen, Switzerland*

Holotype of Yaksha perettii and referred sample, Daza et al. (2020)

Fig. 1 GRS-SRef-060829 33.720 ct

Fig. 2 GRS-Ref-27746 28.193 ct

INTRODUCTION

Amber samples from Myanmar (Burmite) with vertebrate inclusions are rare and only found with the community's effort (Peretti 2020). There is a considerable time-delay between the discovery of special inclusions in the cutting centers late after the recovery of the samples. We call these community effort samples. Most of the samples published in the literature may come from this pool of amber samples. In contrary, certain amber samples can be found directly at the mine, particular rough amber samples with no special paleontological inclusions. These amber samples directly collected at the mine can be used as amber origin reference standards. The analysis of the amber material itself can give an indication of the origin by the comparison of community effort samples and amber origin reference standards.

The methods applied are normally used in a gemological laboratory for the purpose of analyzing gemstones and comprise non-destructive fingerprinting methods, namely Fourier-transform infrared spectroscopy (FTIR) and photoluminescence spectroscopy (PL). FTIR spectroscopy of amber can be applied using a new Attenuated Total Reflection (ATR) method (Musa et al., 2020). This technique allows the analysis of specimens with low to no sample preparation. The latest generation of ATR spectrophotometers are coupled with a microscope in order to select a small area of the specimen and to analyze and map the different IR vibrational modes.

This allows to spatially correlate the measurements with the specimen's morphology. In addition to UV-fluorescence imaging, PL-fluorescence spectroscopy can be applied. This allows to analyze spectroscopically emitted UV-fluorescence.

In this report, we present the analysis of different groups of amber including holotypes and other referred materials (Fig. 1 and Fig. 2) described by Daza et al. (2020) that are found with community effort and compared them to our amber origin reference standards. Selected fingerprinting methods were applied including those reported by Musa et al. (2020). Data was recorded on different layers of the sample and correlated to UV-fluorescence across specimens at the same sample positions. In addition to the spectroscopic fingerprinting techniques, the individual amber specimens were characterized by inclusions of organic materials as well as vertebrate and invertebrate inclusions. These inclusions are also characterized here by microscopic as well as CT-imaging analysis. Even though invertebrate inclusions are not assigned yet, their micro photographic survey provides a good individual characterization of the amber specimens.

The CT-imaging data were processed in 3-diemsional representation to further study vertebrate and invertebrate inclusions in the amber specimens. The 3-diemsional representation data is provided as augmented reality movies that can be generated using the free of charge "GRS AR" app (download at apple store and google play store).

MATERIALS

The studied Burmite amber samples from different mining provinces in Myanmar are summarized in Tab. 1 in the appendix. The samples are separated into 2 groups, community effort recovered polished samples and amber origin reference standards collected as rough pieces directly at the mine. This included the GRS-Ref-28627 (amber with Oculudentavis naga inclusion) which is a sample with a reported origin but not collected directly from a mining spot.

METHODS

Micro-ATR/FTIR Spectroscopy

The FTIR spectra were acquired using a Spotlight 200i micro-ATR (PerkinElmer) coupled with a Frontier FTIR (Fig. 3 and 4). The analyses were performed via a small contact patch between the germanium ATR crystal and the surface of the specimens. The window opening was fixed at 100x100 µm. 256 scans were recorded to increase the signal to noise ratio. The spectra were acquired in a range of 600 to 5000 cm-1. Micro-ATR/FTIR analyses were carried out at a resolution of 2 cm-1 and 4 cm-1. 2 cm-1 was selected in order to highlight differences in smaller bands between different spots on the same specimen. The resolution of 2 cm-1 reduced the signal to noise ratio but in return induced secondary convoluted vibrations. Before each sample acquisition, a background in air was collected at the same conditions. The sample locations for the micro-ATR were selected on the basis of previous UV fluorescence observations.

Photoluminescence spectroscopy

A custom-built photoluminescence system equipped with a quadruple-channel Czerny-Turner spectrometer was used to analyzing the amber samples using a 405 nm laser source (Fig. 5 and 6). PL measurements were performed in a wavelength range from 405 to 1100 nm range. The amber was measured with 2 different lasers, 405nm (ultra-violet) and 532 nm (green) at room temperature and cooled with liquid nitrogen (LN). Only the 405nm laser source without cooling to LN temperatures was non-destructive. Time of measurement was optimized to 4 seconds. Longer measurements created craters that resulted in reduction of signal due to melting of amber.

UV Fluorescence Imaging

The UV-fluorescence images were acquired using a UVP UVGL-58 wood lamp (Analytik Jena) and a EOS R camera (Canon). The wood lamp was equipped with a long-wave lamp (365 nm) and short-wave lamp (254 nm) both with a power of 8 W. EOS R camera used a 24-105 mm lens and the amber samples were placed in a dark box.

RESULTS

The amber sample containing Oculudentavis naga shows differences in fluorescence of weak greyish-blue and strong chalky-blue with very small diffuse orangy fluorescent zones, separating the different amber flows. The flows have a very distinct separation in one area with abundant fluid inclusion bubbles. Different flows are characterized by accumulation of invertebrate, blackish ash-like particles and other debris, correlated with different flows (Fig. 7 and 8). Reference materials from Aungbar published by Musa et al. (2020) show the same characteristics in the microscopic examination with the exception of larger areas with orange fluorescence. The Aungbar samples from our reference collections contained amber flows with enrichment of fluid inclusion bubbles. Those were also found in the amber flows of Oculudentavis naga.

FTIR spectra were recorded according to the new method reported by Musa et al. (2020). Multiple Burmite samples from different mining areas in Myanmar (Peretti 2020) were measured. These include the mining areas of Khamti, Hti Lin, Zee Phyue Kone and Aungbar representing some of the amber mines all over Myanmar from the PME collection. In Fig. 9 to 19 the FTIR spectra of community effort samples including Oculudentavis naga GRS-Ref-28627 and Yaksha perettii SRef-060829 and amber origin reference standards from the different mining areas are presented.

Fig. 3 Attenuated Total Reflection (ATR) spectroscopy for non-destructive analysis of amber in mm sample resolution at the Laboratory of GRS Thailand in Bangkok.

Fig. 4 A germanium ATR crystal was used with direct contact to the surface of the amber specimens. The method requires liquid nitrogen cooling for the microscope unit detector.

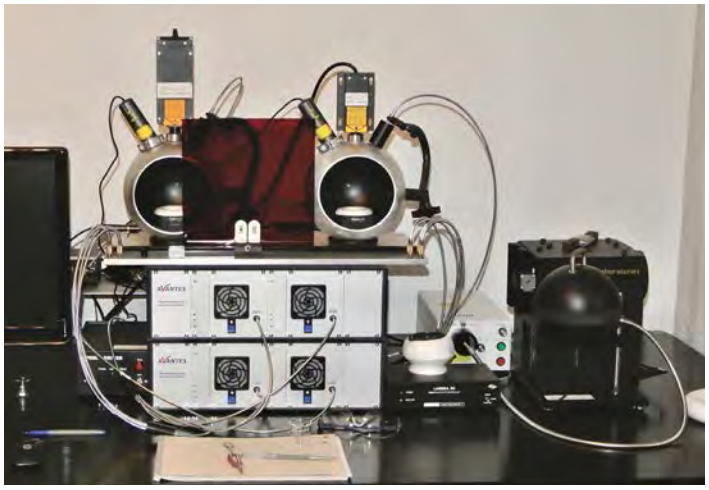

Fig. 5 A look at the GRS research laboratory instrumentation in Switzerland, Hong Kong and Thailand. On the left side the custom-built photoluminescence analysis system with 2 laser sources (405 and 532 nm) is shown. The right side shows a close-up of one analyzed head with a 532 nm laser illuminating a sample.

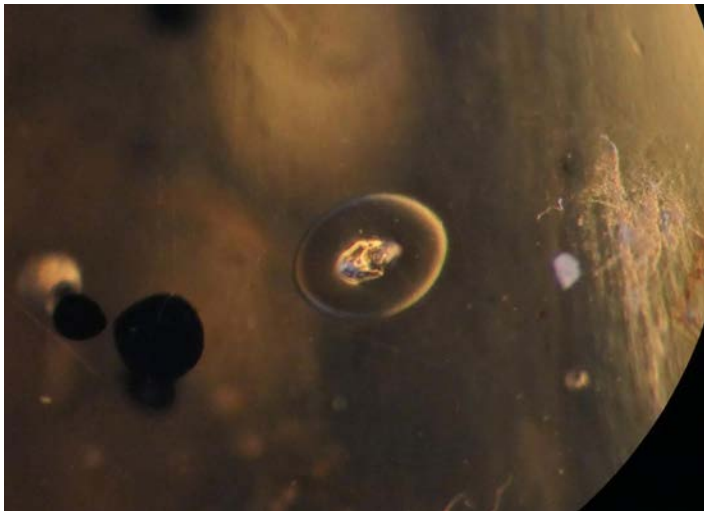

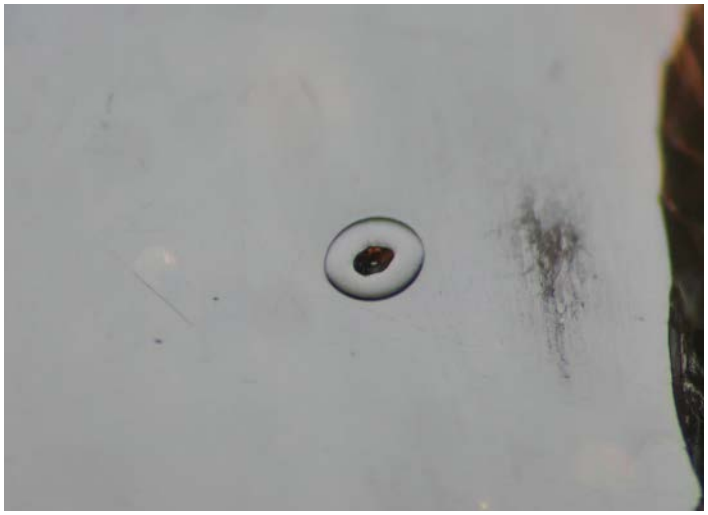

Fig. 6 Laser marks as a result of PL measurement with a 405 nm laser. After 5 seconds excitation GRS-Ref-28627-Oculudentavis naga. Diameter of crater is approximately 20 µm.

Fig. 7 Macro-photo in transmitted light of Oculudentavis naga in amber GRS-Ref-28627 with dimensions 53.11 x 23.07 x 10.06 mm showing vertebrate and invertebrate inclusions as well as some amber flows marked by bands of bubbles. In the upper part of the picture there is a curved band of bubbles marking the border between different amber flows.

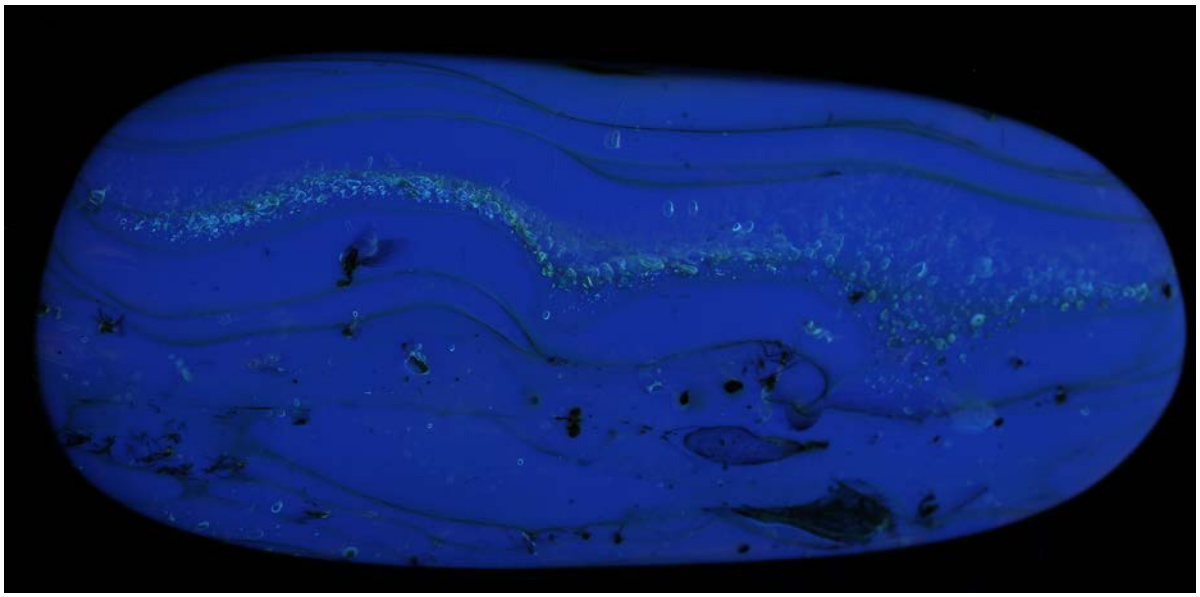

Fig. 8 UV fluorescence image of same amber as in Fig. 3 showing chalky-blue UV fluorescence when exposed to long-wave (365 nm) UV light. The band of bubbles are visible as in Fig. 3. In addition, the multiple amber flows are much better defined than in the picture obtained in transmitted light. The Oculudentavis naga sample has been measured with the same instrumentation as published by Musa et al. (2020) and compared to the measurements of their samples.

FTIR fingerprint range of Burmese amber from different mines
(acquired on samples from the GRS reference collection)

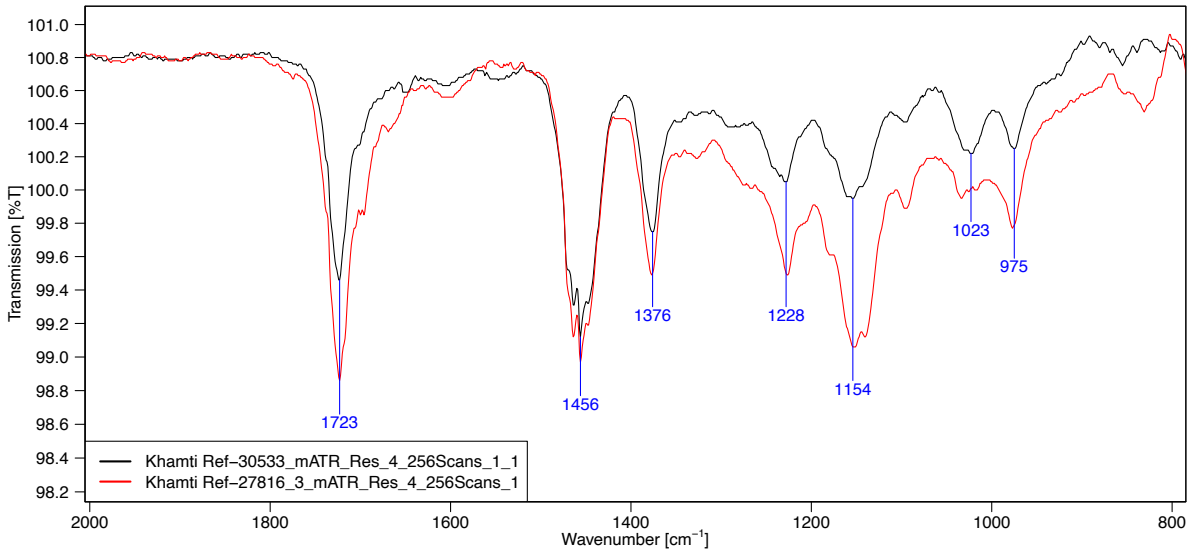

Fig. 9 Detail of the FTIR fingerprint range of Burmese Amber from Khamti. GRS-Ref-30533 (black) and GRS-Ref-27816 (red)

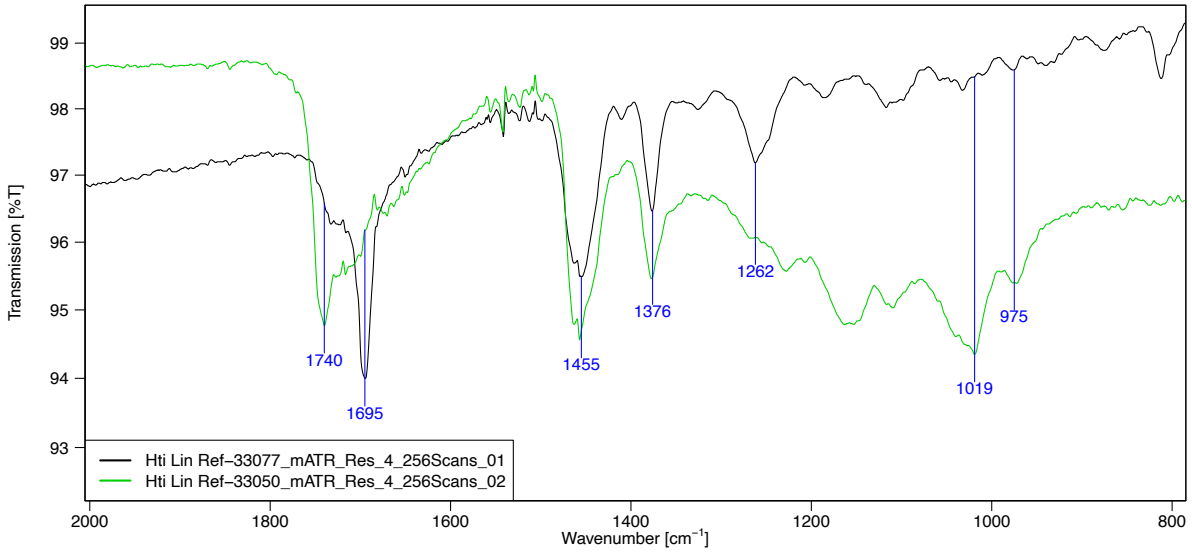

Fig. 10 Detail of the FTIR fingerprint range of Burmese Amber from Hti Lin. GRS-Ref-33077 (black) and GRS-Ref-33050 (green)

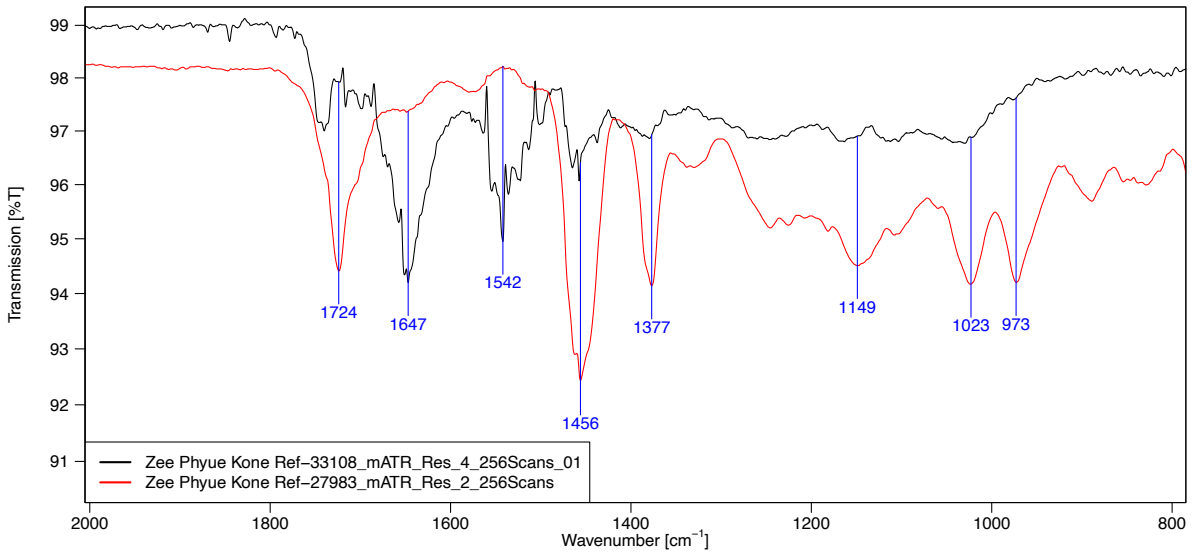

Fig. 11 Detail of the FTIR fingerprint range of Burmese Amber from Zee Phyue Kone. GRS-Ref-28983 (black) and GRS-Ref-33108 (red)

FTIR fingerprint range of Burmese amber from different mines comparison with holotypes
(acquired on samples from the GRS reference collection)

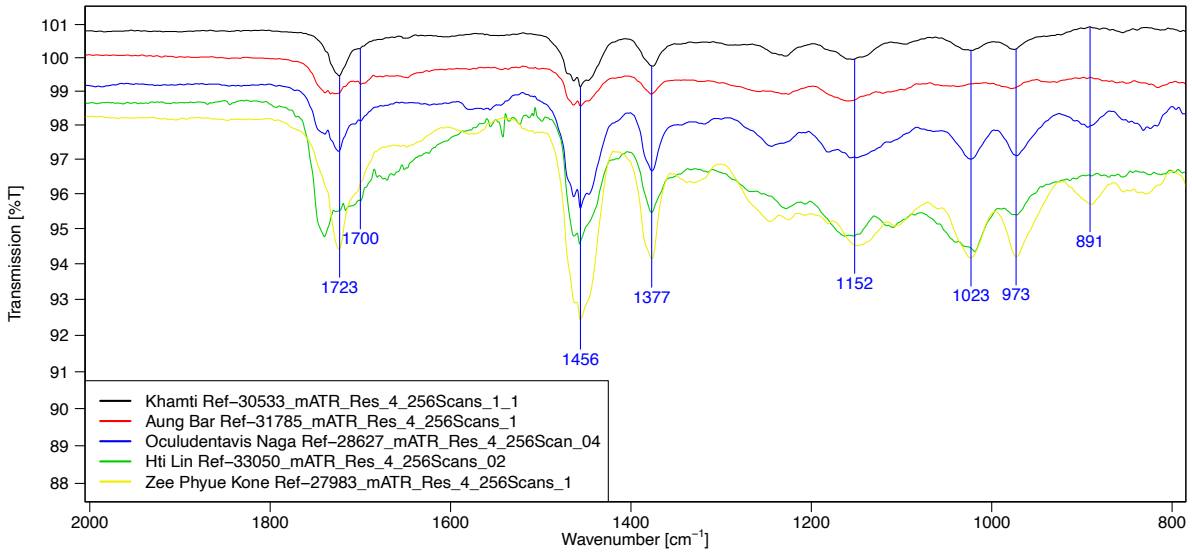

Fig. 12 Overlap of spectra of Oculudentavis naga (GRS-Ref-28627, orange) with spectra of amber from Zee Phyue Kone (GRS-Ref-28983, black), Hti Lin (GRS-Ref-33050, red), Khamti (GRS-Ref-30533, blue) , and Aung Bar (GRS-Ref-31785, green).

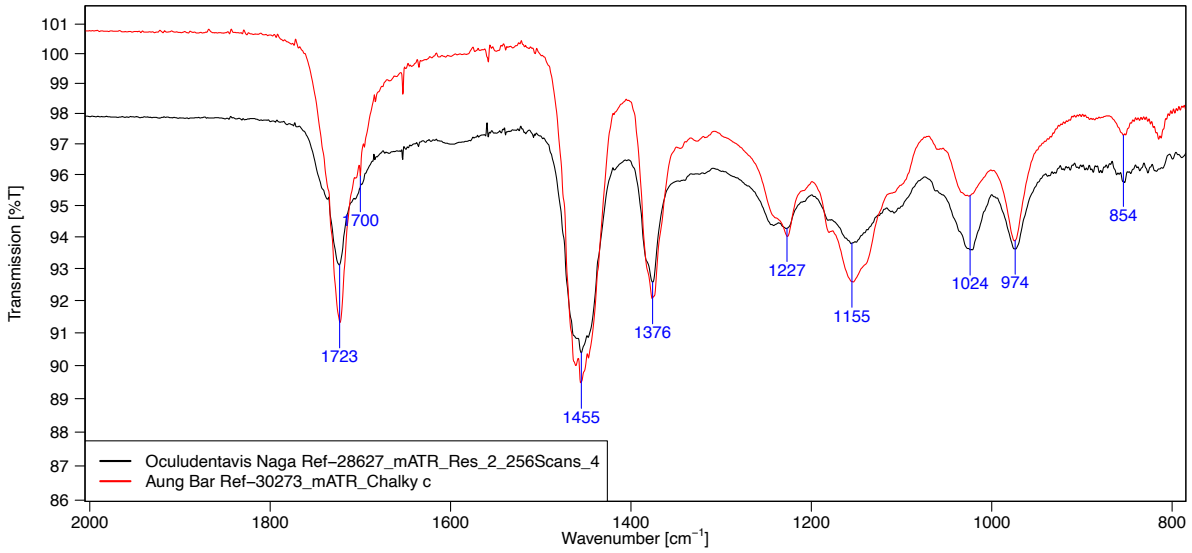

Fig. 13 Overlap of spectra of Oculudentavis naga with a reference sample from Aungbar. GRS-Ref-30273 (red) and GRS-Ref-28627 (black). The difference in ratio of the 1024 cm-1 and 975 cm-1 can be explained by variations of different amber flows (see Fig. 5).

FTIR fingerprint range of Burmese amber from different mines comparison with holotypes
(acquired on samples from the GRS reference collection)

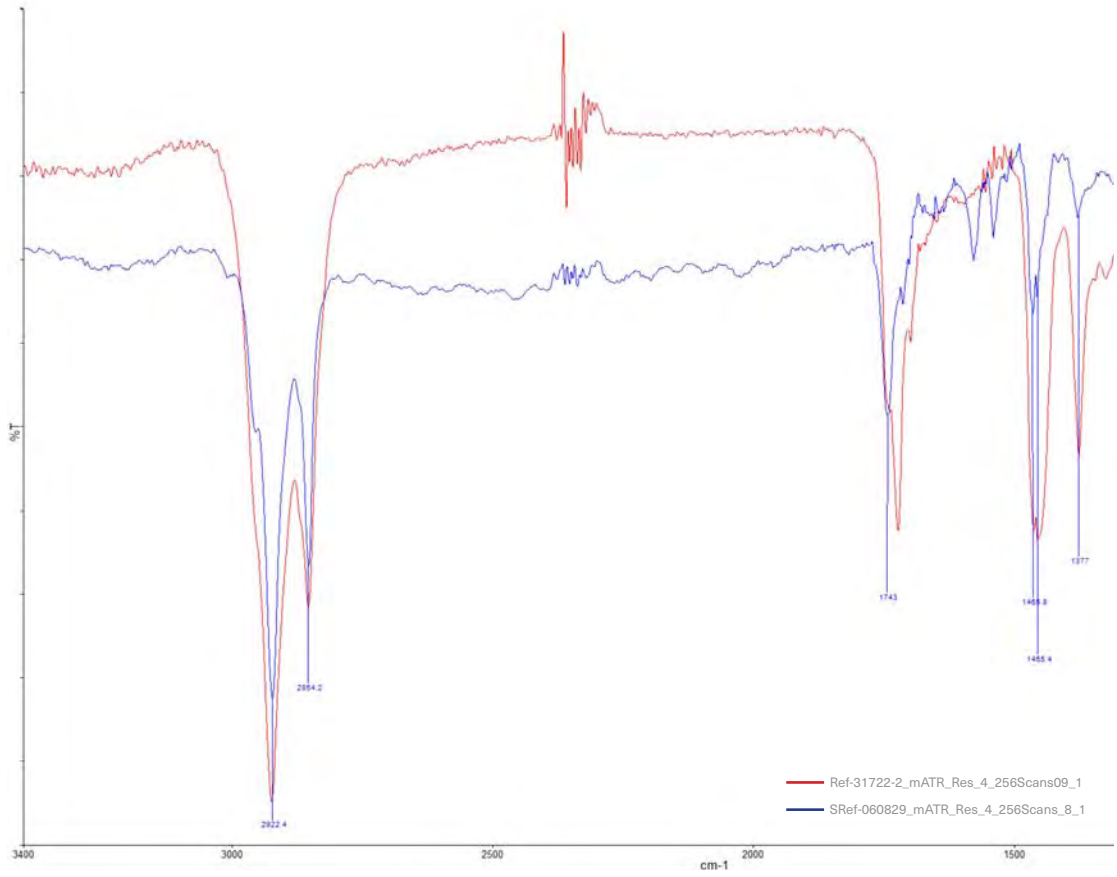

Fig. 14 mATR overlap of GRS-SRef-060829 Yaksha perettii with GRS-Ref-31722-2 (full range)

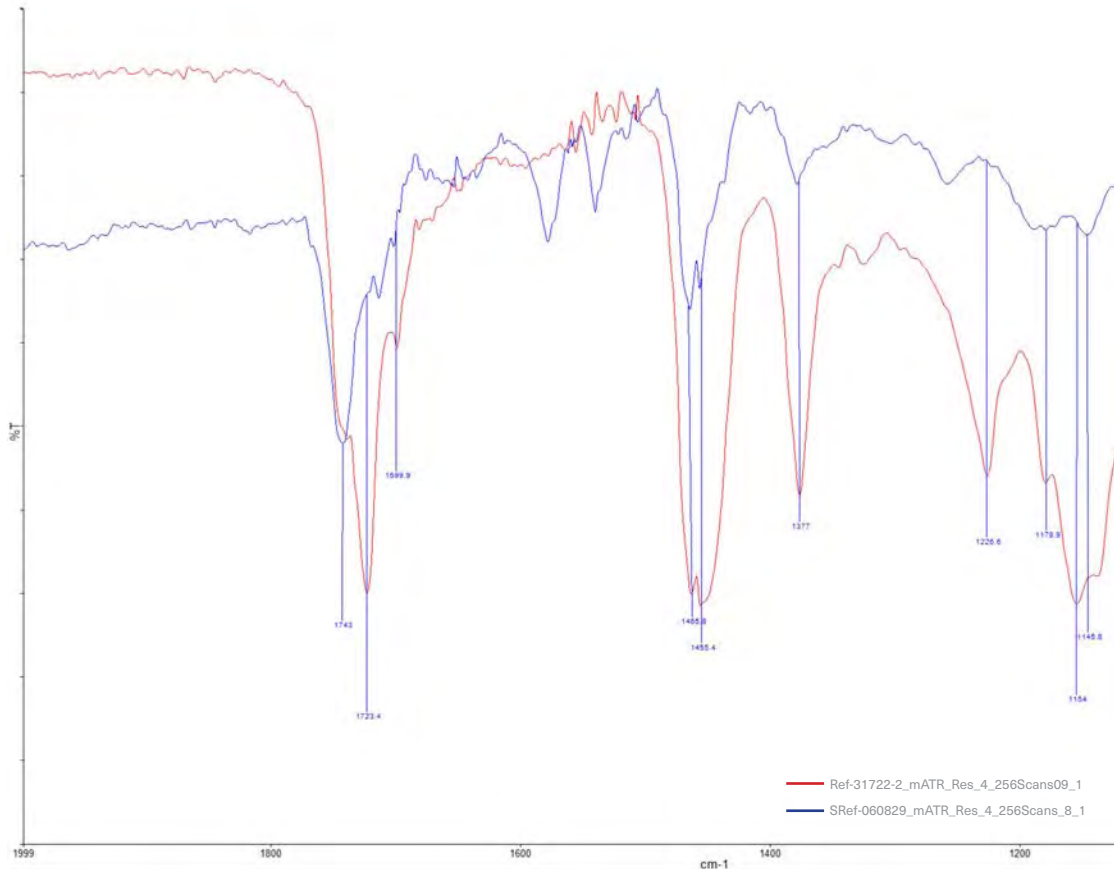

Fig. 15 mATR overlap of GRS-SRef-060829 Yaksha perettii with GRS-Ref-31722-2 (selected range)

FTIR fingerprint range of Burmese amber holotypes

(acquired on samples from the GRS reference collection)

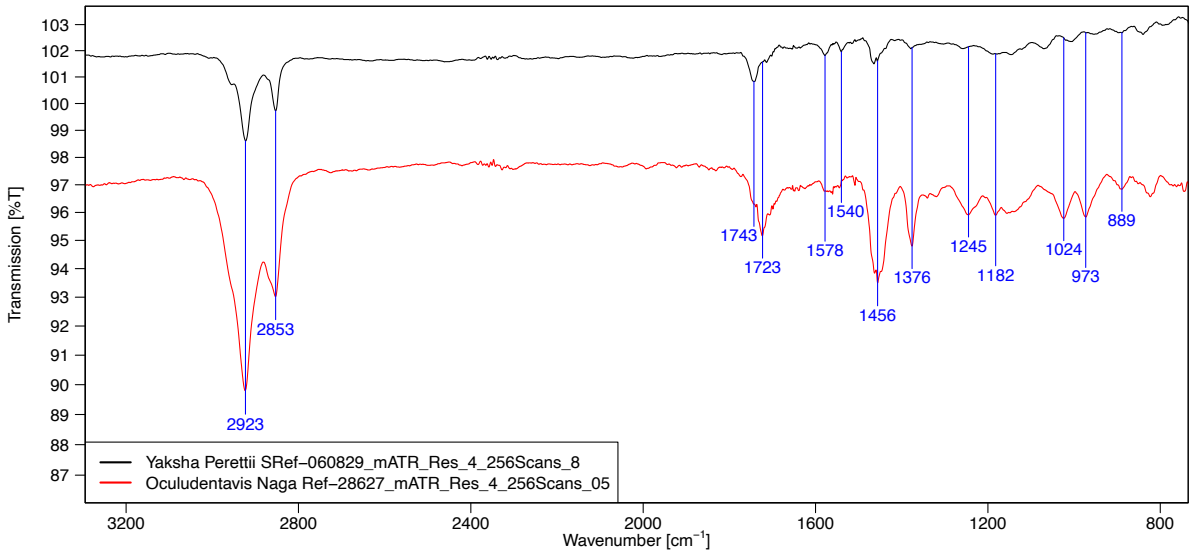

Fig. 16 mATR overlap of GRS-SRef-060829 Yaksha perettii (black) and GRS-Ref-28627 Oculudentavis Naga (red)

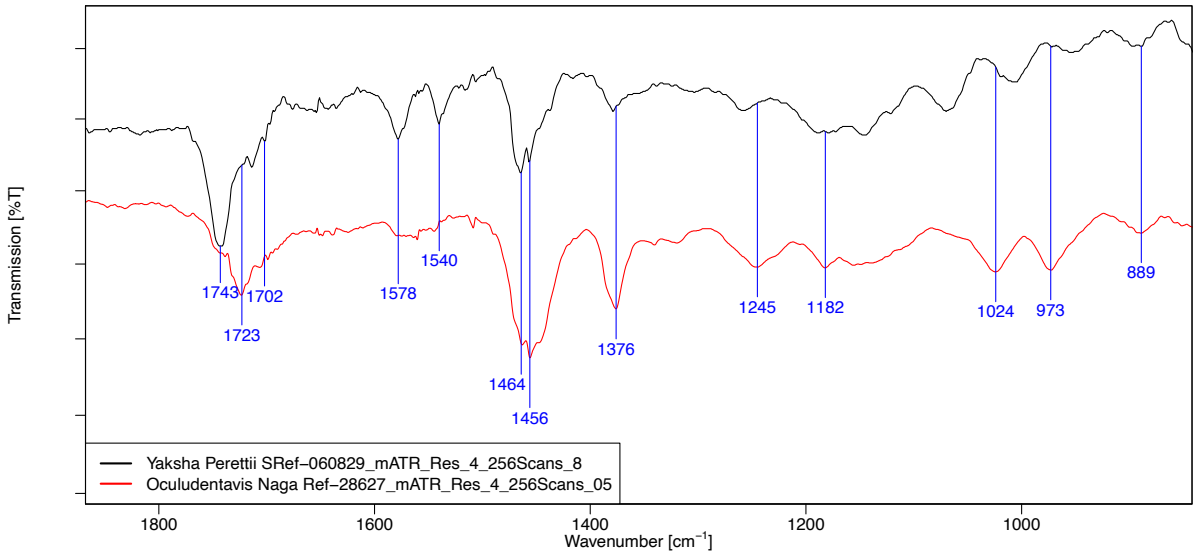

Fig. 17 Detail of the FTIR fingerprint range of GRS-SRef-060829 Yaksha perettii (black) and GRS-Ref-28627 Oculudentavis Naga (red)

FTIR fingerprint range of Burmese amber holotype and referred sample
(acquired on samples from the GRS reference collection)

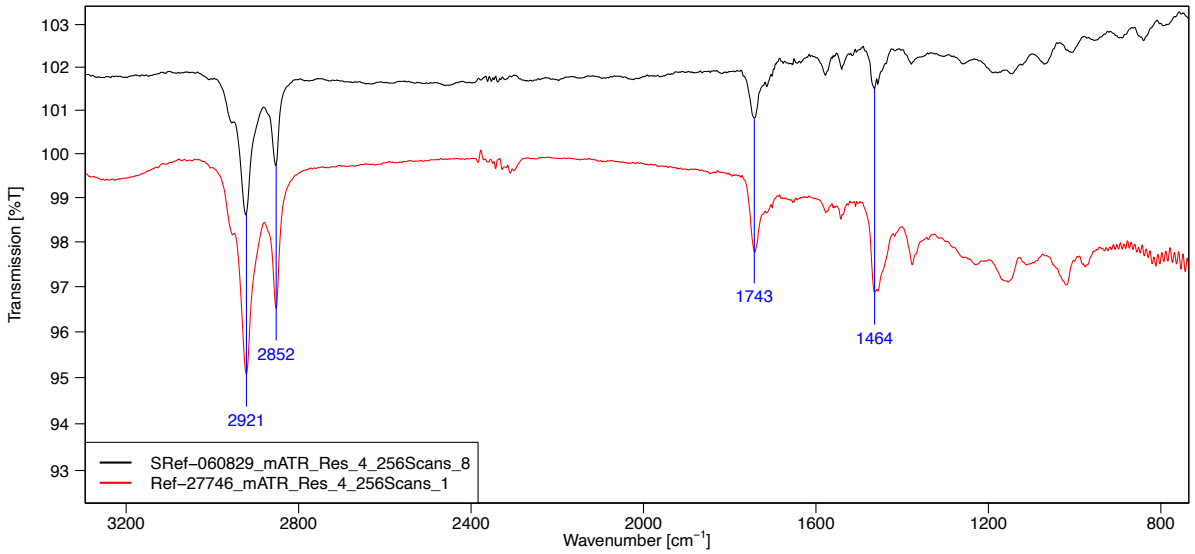

Fig. 18 mATR overlap Yaksha perettii SRef-060829 and Referred Ref-27746

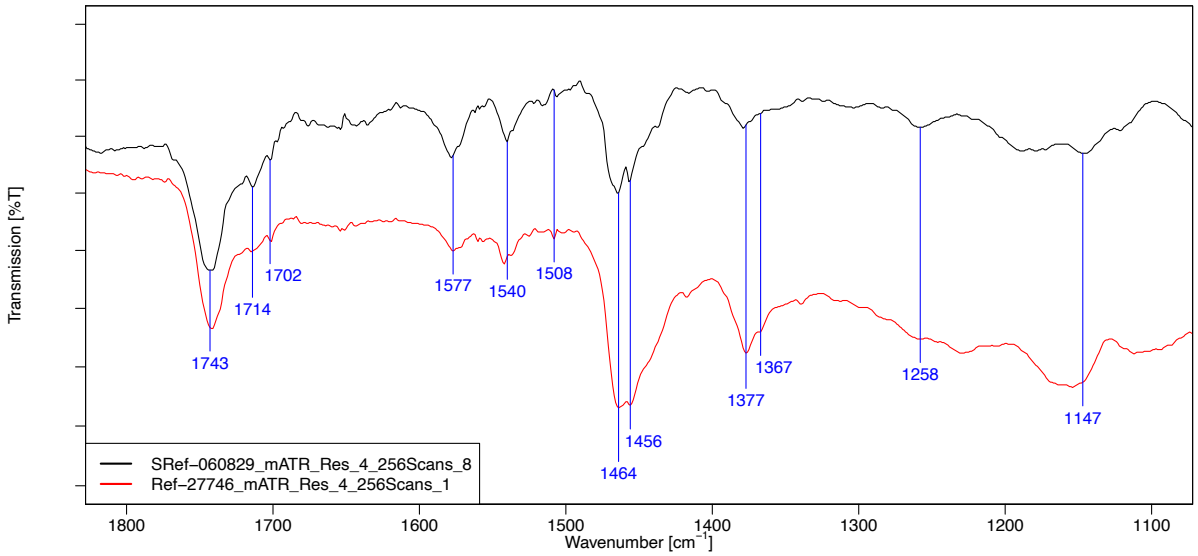

Fig. 19 mATR overlap Yaksha perettii SRef-060829 and Referred Ref-27746

Photoluminescence of Burmese amber holotypes and reference samples

(acquired on samples from the GRS reference collection)

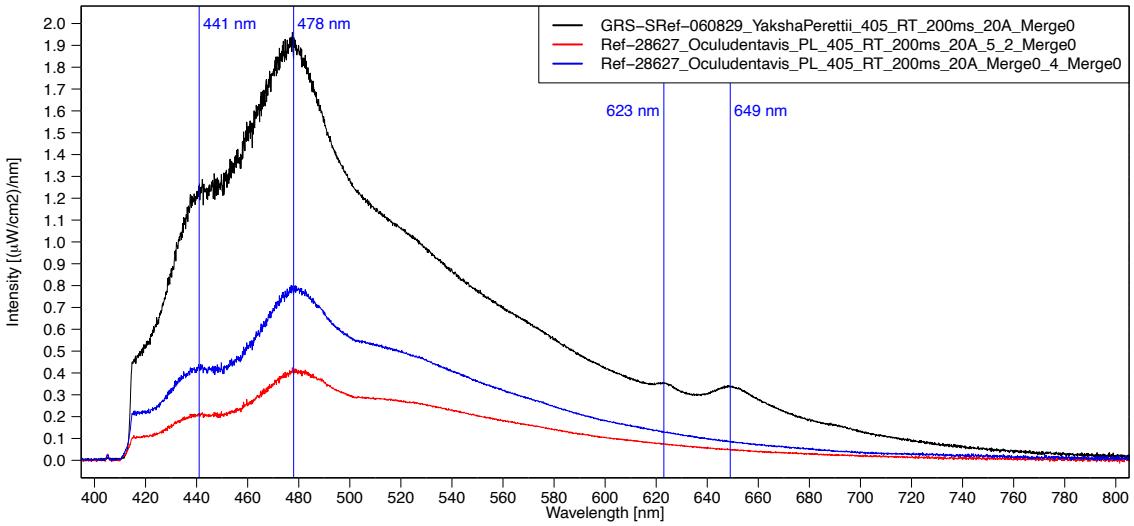

Fig. 20 Photoluminescence spectra of GRS-SRef-060829 Yaksha perettii (red) and GRS-Ref-28627 Oculudentavis naga (green, turquoise).

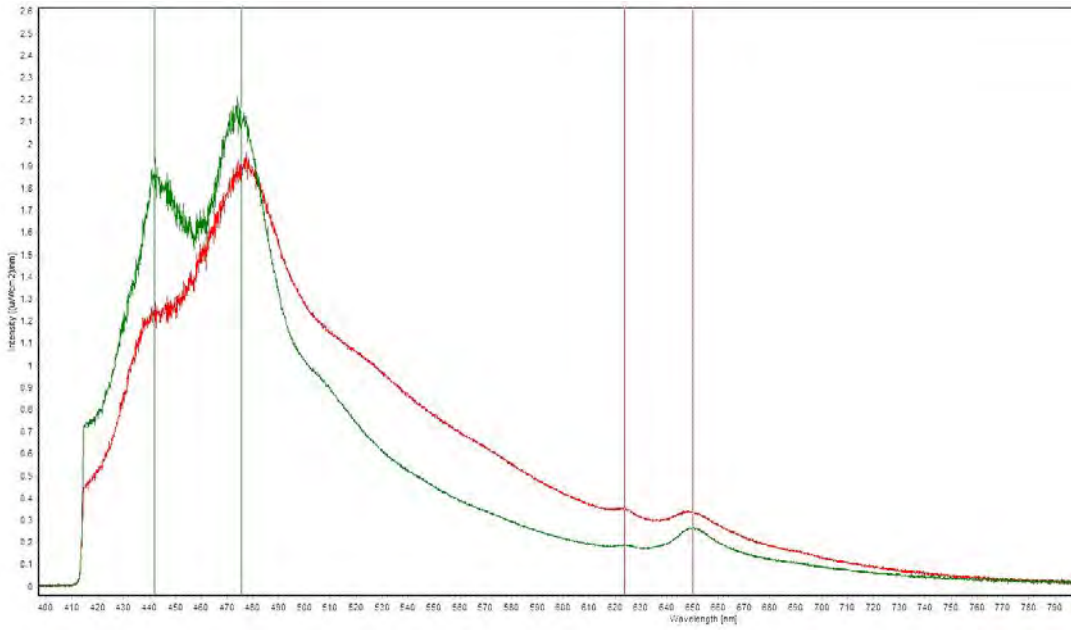

Fig. 21 Overlap_GRS-SRef-060829_Yaksha perettii_and_GRS-Ref-31772_Aungbar_Tanai_Yar Mut

RESULTS AND INTERPRETATION

The analysis of amber matrix as well as inclusions provided a large data set of characteristics to individually describe and allocate different amber samples. Particularly, the holotypes and referred materials were characterized and provide a good data set to be compared with other known materials. The comparisons are shown in Fig. 12 to 19. Comparing FTIR data of community discovered amber and amber origin reference standards provide many overlapping results. However, when PL spectroscopy is included, more specific matches with origin reference standard materials can be found (Fig. 20 and 21). The extensive analysis campaign shows that GRS-Ref-28627 (Oculudentavis Naga) is corresponding to the blue fluorescence type FTIR spectra of an Aungbar origin reference standard. This sample has also been described by Musa et al. 2020 (see Fig. 22). The FTIR samples of holotypes including Yaksha perettii and Oculudentavis naga were most similar to Burmite amber from Aungbar and Zee Phyue Kone both located im the Hukwaung valley. PL-spectroscopy in addition allowed to localize them with a particular origin reference standard in the Aungbar mining area.

Invertebrate identification in the Oculudentavis naga sample may provide potential for the conclusion of the sample being of the origin from the Hukwaung valley that includes the Aungbar mines but also others in that area, such as Zhee Phy Gone etc. (see Peretti et al., 2020).

Regarding the PL fluorescence data, 7 different types were distinguished. Hti Lin amber samples are characterized by very low PL intensities, and Khamti amber has PL spectra that were not observed in other origins. Aungbar occupies mostly 2 types of PL spectra. In comparison to published PL spectra in the literature, the same type of spectra were found in the Aungbar and Zee Phy Gone samples (Hukwaung valley) as published in the literature for the same origin (Zhang et al 2020). The correlation of spectra with different Amber colors was not observed though. These sets of analysis are only the first testing series that can let us understand the potential of the method. A large scale survey of the different types of Amber in different layers in hundreds of different mining spots will deliver a more clear picture of how powerful the method will be for more precise origin determination. Our preliminary analysis promises a good variability of observations for different mining areas, particularly if all methods of fingerprinting including FTIR, fluorescence as well as PL spectroscopy are considered. Particularly if the observations of different methods are applied as measurements of variations layer by layer of the different amber flows. It is therefore necessary to use micro analytical methods that allow spatial resolution of areas in the mm range.

Based on the analysis presented here, the origin of the samples being reported from the Aungbar is not in contradiction with the findings of this comparison study. The origin from the Hukwaung valley is quite well established.

ACKNOWLEDGEMENTS

We thank Saleem Micheal of GRS (Thailand) Co. Ltd, Bangkok and Claudio Alessandri and Andre Huber of GRS Gemresearch Swisslab AG, Switzerland for measuring the samples and for acquiring the macrophotography and UV images. The Peretti Museum Foundation for providing the samples.

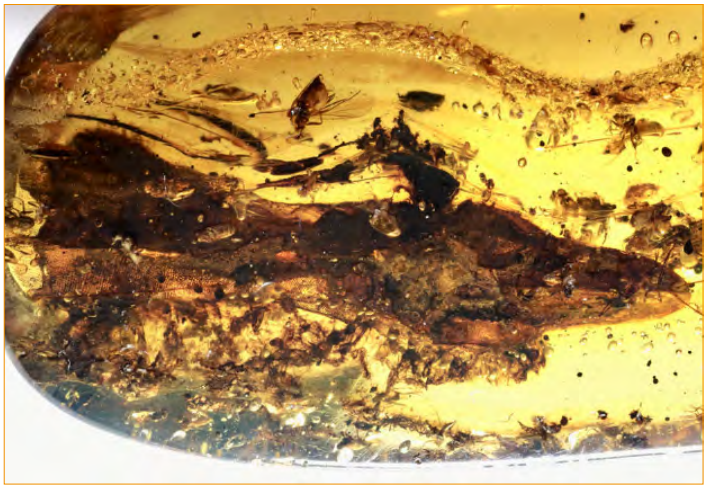

Fig. 22 Inclusions in amber GRS-Ref-28627 of vertebrates (Oculudentavis Naga) and invertebrates (diptera: phoridae platypezidae, ceratopogonidae; Coleoptera: elateriforme). In the upper part of the picture there is a curved band of bubbles marking the border between different amber flows.

LITERATURE

Bolet, A. Stanley, E. L. Daza, J. D. Salvador Arias, J. Čerňanský, A. Vidal-García, M. Bevitt, J. J. Peretti, A. Evans, S.E. "Unusual morphology in the mid-Cretaceous lizard Oculudentavis". Current Biology. 31 (15): 3303–3314 (2021).

Daza, J.D. Stanley, E.L. Bolet, A. Bauer, A.M. Salvador Arias, J. Čerňanský, A. Bevitt, J.J. Wagner, P. Evans, S.E. "Enigmatic amphibians in mid-Cretaceous amber were chameleon-like ballistic feeders". Science. 370 (6517): 687–691 (2020).

Kosmowska-Ceranowicz, B. Vavra, N. "Burmite, Cedarite". In: B. Kosmowska-Ceranowicz, N. Vavra. Atlas infrared spectra of the world's resins. Holotype Characteristics. Warsaw: Polish Academy of Sciences Museum of the Earth. 2015. 32.

Musa, M. Kaye, T. Bieri, W. Peretti, A. "Burmese Amber Compared Using Micro-Attenuated Total Reflection Infrared Spectroscopy and Ultraviolet Imaging". Appl Spectrosc. 75 (7):839-845 (2021).

Peretti, A. Ethical guidelines for Burmese amber acquisitions. Journal of Applied Ethical Mining of Natural Resources and Paleontology 1, 4–78 (2020).

APPENDIX 1

Number	Weight (ct)	Description	Origin	Mining Area
GRS-Ref-28627	33.275	Burmese Amber	Burma (Myanmar)	Aungbar
GRS-Ref-31785	63.473	Burmese Amber	Burma (Myanmar)	Aungbar
GRS-Ref-30188	38.387	Burmese Amber	Burma (Myanmar)	Aungbar
GRS-Ref-30273	21.909	Burmese Amber	Burma (Myanmar)	Aungbar
GRS-Ref-30933	12.961	Burmese Amber	Burma (Myanmar)	Aungbar
GRS-Ref-30966	23.202	Burmese Amber	Burma (Myanmar)	Aungbar
GRS-Ref-30533	63.63	Burmese Amber	Burma (Myanmar)	Khamti
GRS-Ref-27816	5.748	Burmese Amber	Burma (Myanmar)	Khamti
GRS-Ref-33050	4.807	Burmese Amber	Burma (Myanmar)	Tilin Area - Kyar Khe
GRS-Ref-33077	0.439	Burmese Amber	Burma (Myanmar)	Tilin Area - Nyaung
GRS-Ref-33111	3.376	Burmese Amber	Burma (Myanmar)	Zee Phyu Kone
GRS-Ref-28983	6.021	Burmese Amber	Burma (Myanmar)	Zee Phyue Kone
GRS-Ref-33108	2.573	Burmese Amber	Burma (Myanmar)	Zee Phyue Kone
GRS-Ref-27746	28.193	Burmese Amber	Burma (Myanmar)	Aungbar

Tab. 1 List of GRS reference samples use for this report.

APPENDIX 2: DATA COLLECTION OF GRS-REF-28627

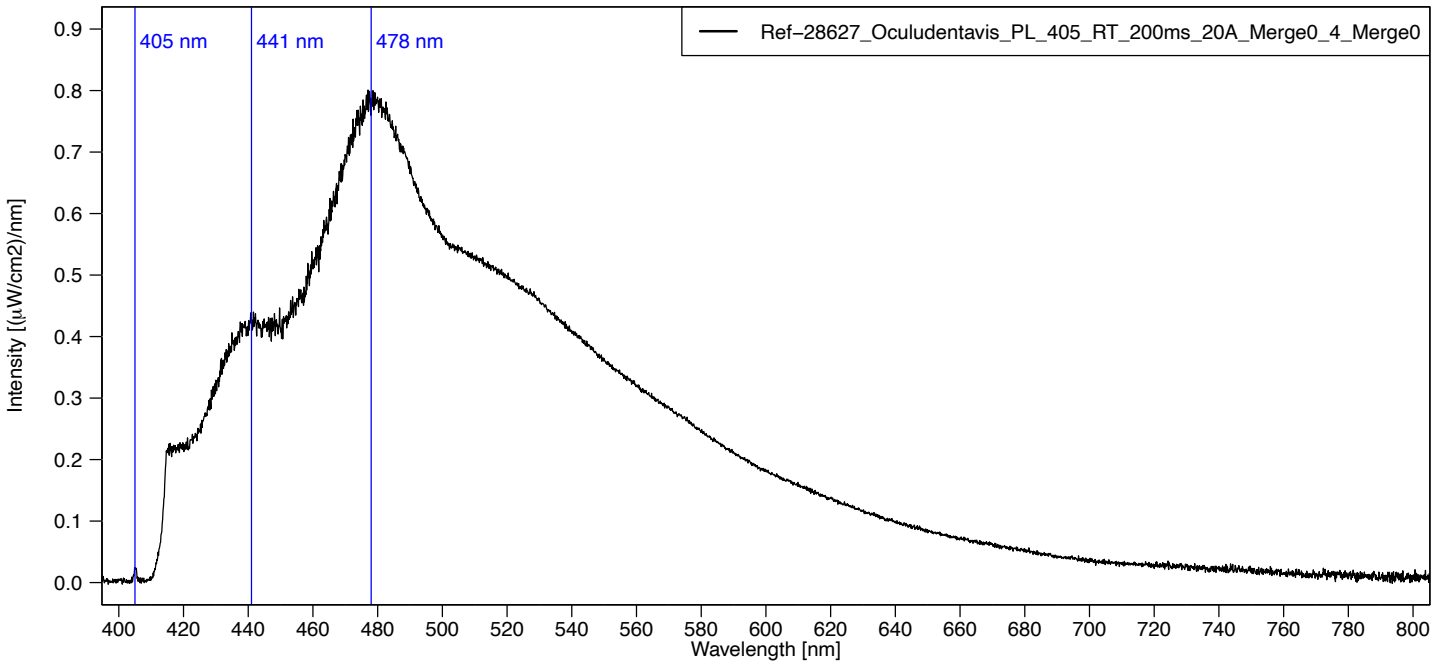

Fig. 23 Photoluminescence spectrum of GRS-Ref-28627 "Oculudentavis Naga". 405 nm laser source at room temperature. Excitation time: 4 seconds. The spectrum shows two luminescence centres in the violet-to-blue region (at 437 and 477 nm). Also visible in the spectra is the laser emission line at 405 nm.

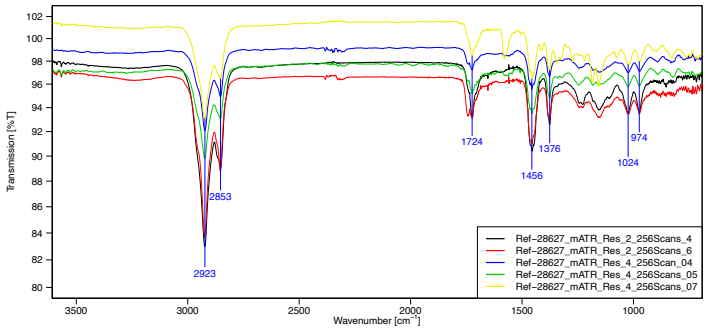

Fig. 24 Spectra of GRS-Ref-28627 (Oculudentavis Naga) measured at 5 different spots.

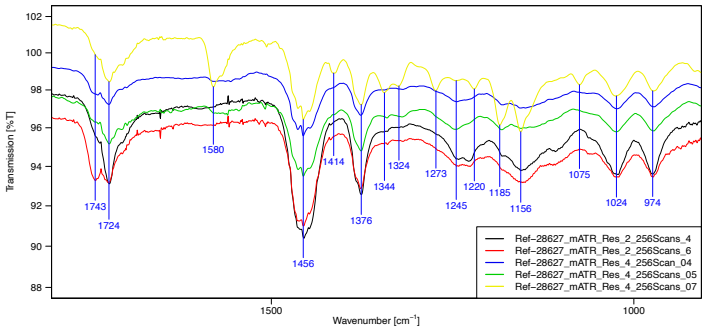

Fig. 25 Detail of the fingerprint range of Fig. 6

Fig. 24 and 25 (6 and 7) Overlap in the fingerprint range of the micro-ATR spectra carried out on Ref-28627 sample in the chalky-blue fluorescence area. Homogeneous FTIR spectra band distributions were found.

Fingerprint FTIR variations in different amber flows (GRS-Ref-28627). Characteristics of the FTIR spectra are:

A main peak at 1725 cm^{-1}, a shoulder at 1743 cm^{-1}, presence or absence of 1580 cm^{-1}, strong 1455 cm^{-1} with side shoulders, 1377cm^{-1} with variation in intensity, presence or absence of 1345 cm^{-1} and 1325 cm^{-1}, presence or absence of 1274 cm^{-1}, variation of relative intensity of the 1184 cm^{-1} and 1156 cm^{-1}, presence or absence of 1076 cm^{-1}, presence of 1025 cm^{-1} and 975 cm^{-1} with almost no change in relative ratio. The absence of a variation of the ratio 1025 cm^{-1} and 975 cm^{-1} is explained by the fact that the orangy fluorescence zone was not present.

Long-wave UV

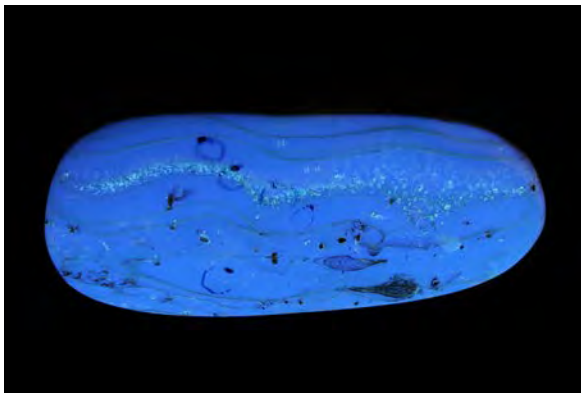

Fig. 26: 4 sec, f/14, ISO 200

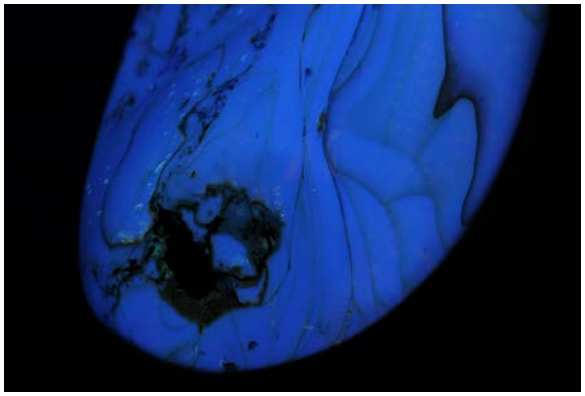

Fig. 28: 5 sec, f/14, ISO 200

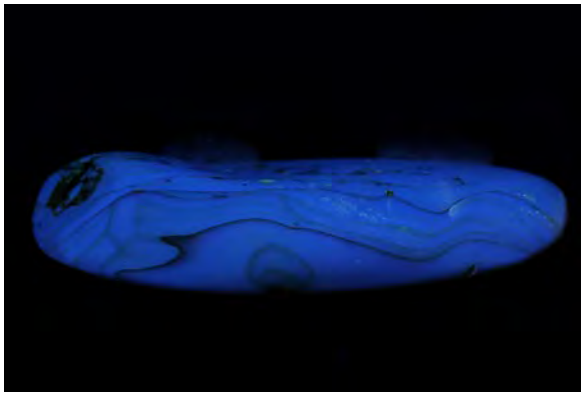

Fig. 30: 2.5 sec, f/14, ISO 200

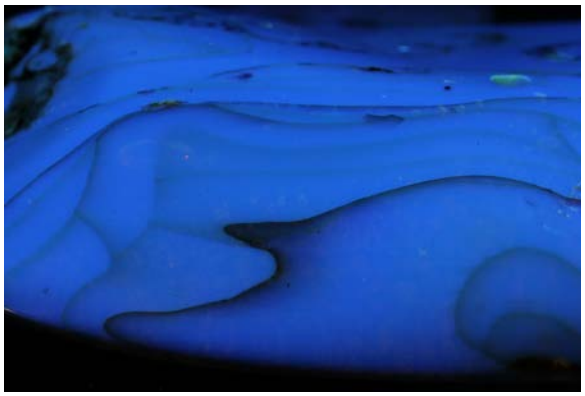

Fig. 31: 3 sec, f/13, ISO 200

Short-wave UV

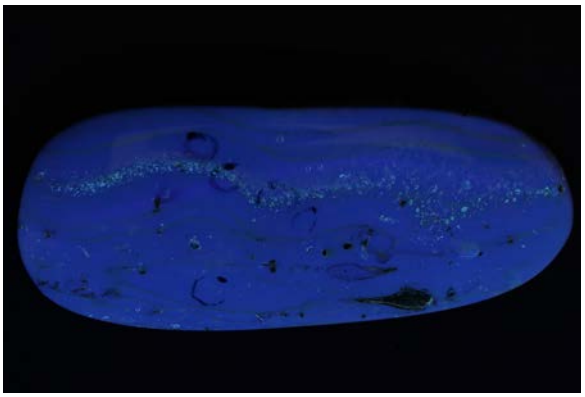

Fig. 27: 20 sec, f/14, ISO 200

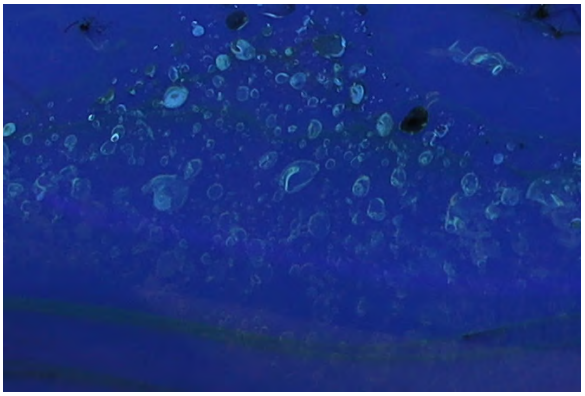

Fig. 29: 20 sec, f/14, ISO 200

Fig. 26-31: Long-wave UV (365 nm) and short-wave UV (254nm) images of amber sample GRS-Ref-28627 (with Oculudentavis naga inclusion). The images were taken with a Canon EOS R camera using a 24-105 mm lens. The images show internal structures of the amber related to different amber flows. The fluorescence is dominated by blue fluorescence with variable intensities and very small orangy bands. Different parts of the sample are shown (reverse and front side of the elongated piece).

APPENDIX 3: IDENTIFICATION OF INSECT INCLUSIONS GRS-REF-28627

The following insects have been identified as a preliminary effort. The exact taxonomic identification is currently in progress and will be updated as soon as it is available.

Fig. 32: Coleoptera: Staphylinidae: Scydmaeninae

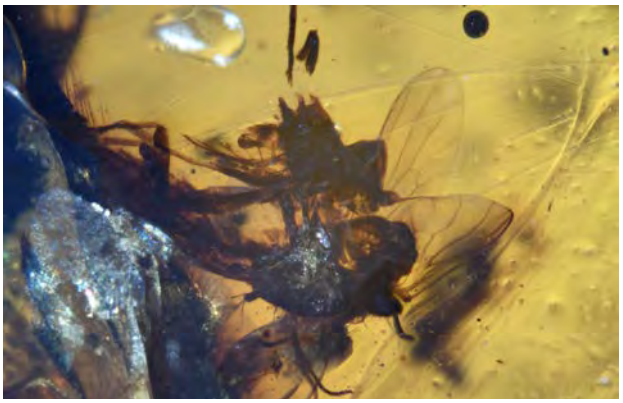

Fig. 33: Diptera: Brachycera: Empidoidea

Fig. 34: Arachnida: Araneae

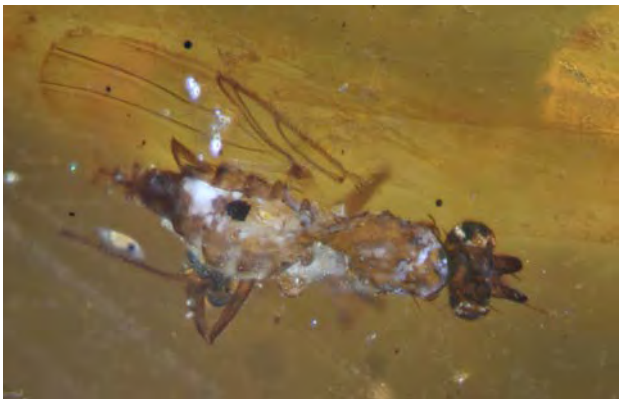

Fig. 35: Diptera: Phoridae

Fig. 36: Diptera: Phoridae and other Diptera: Brachycera

Fig. 37: Diptera: Phoridae

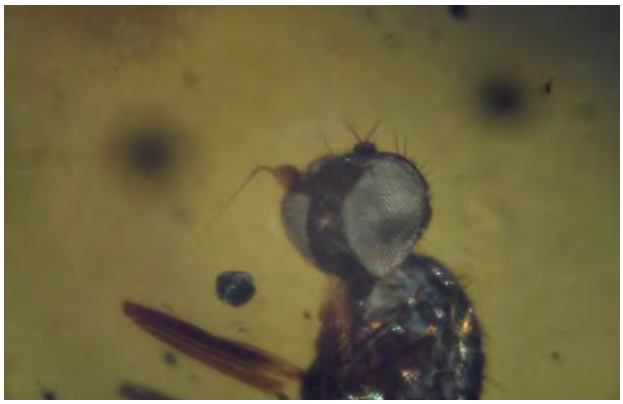

Fig. 38: Diptera: Brachycera: Empidoidea

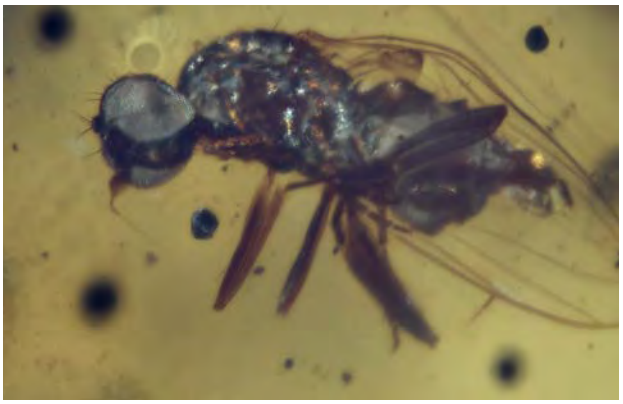

Fig. 39: Diptera: Brachycera: Empidoidea

APPENDIX 3: IDENTIFICATION OF INSECT INCLUSIONS GRS-REF-28627

The following insects have been identified as a preliminary effort. The exact taxonomic identification is currently in progress and will be updated as soon as it is available.

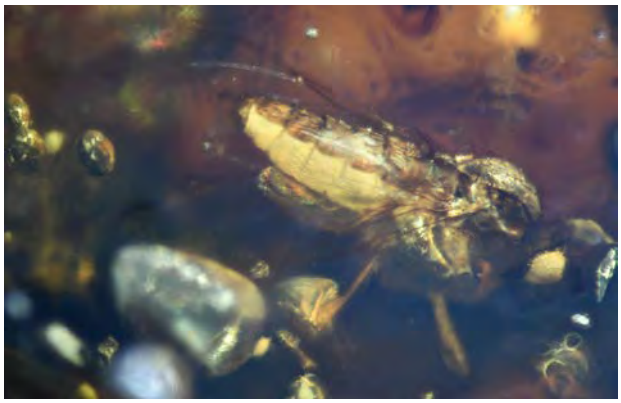

Fig. 40: Diptera: Brachycera: Empidoidea

Fig. 41:

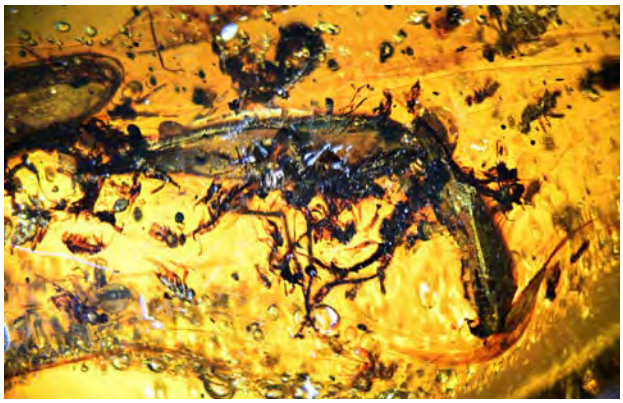

Fig. 42:

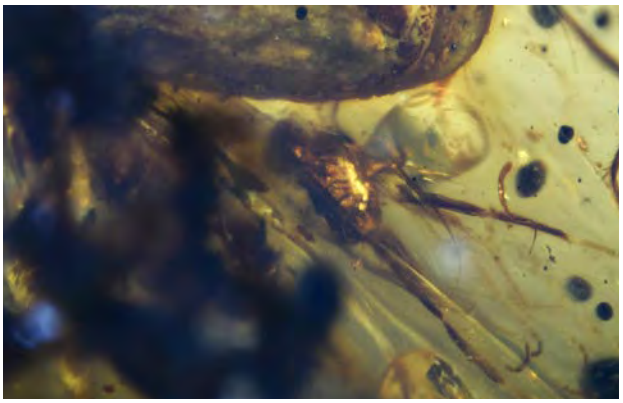

Fig. 43:

Fig. 44:

Fig. 45:

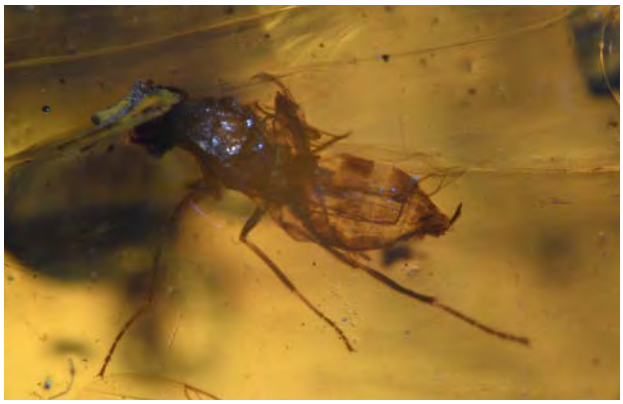

Fig. 46:

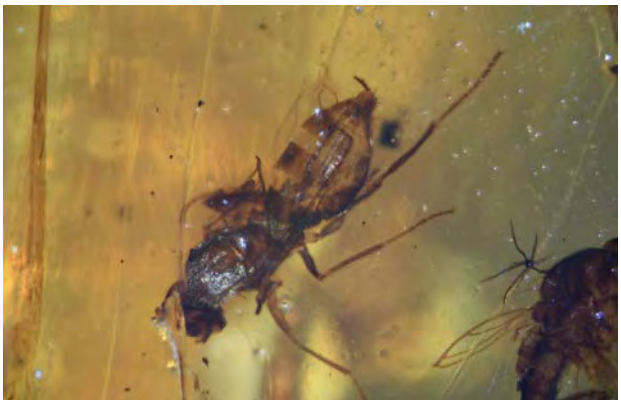

Fig. 47:

APPENDIX 4: IMAGES OF GRS-REF-28627

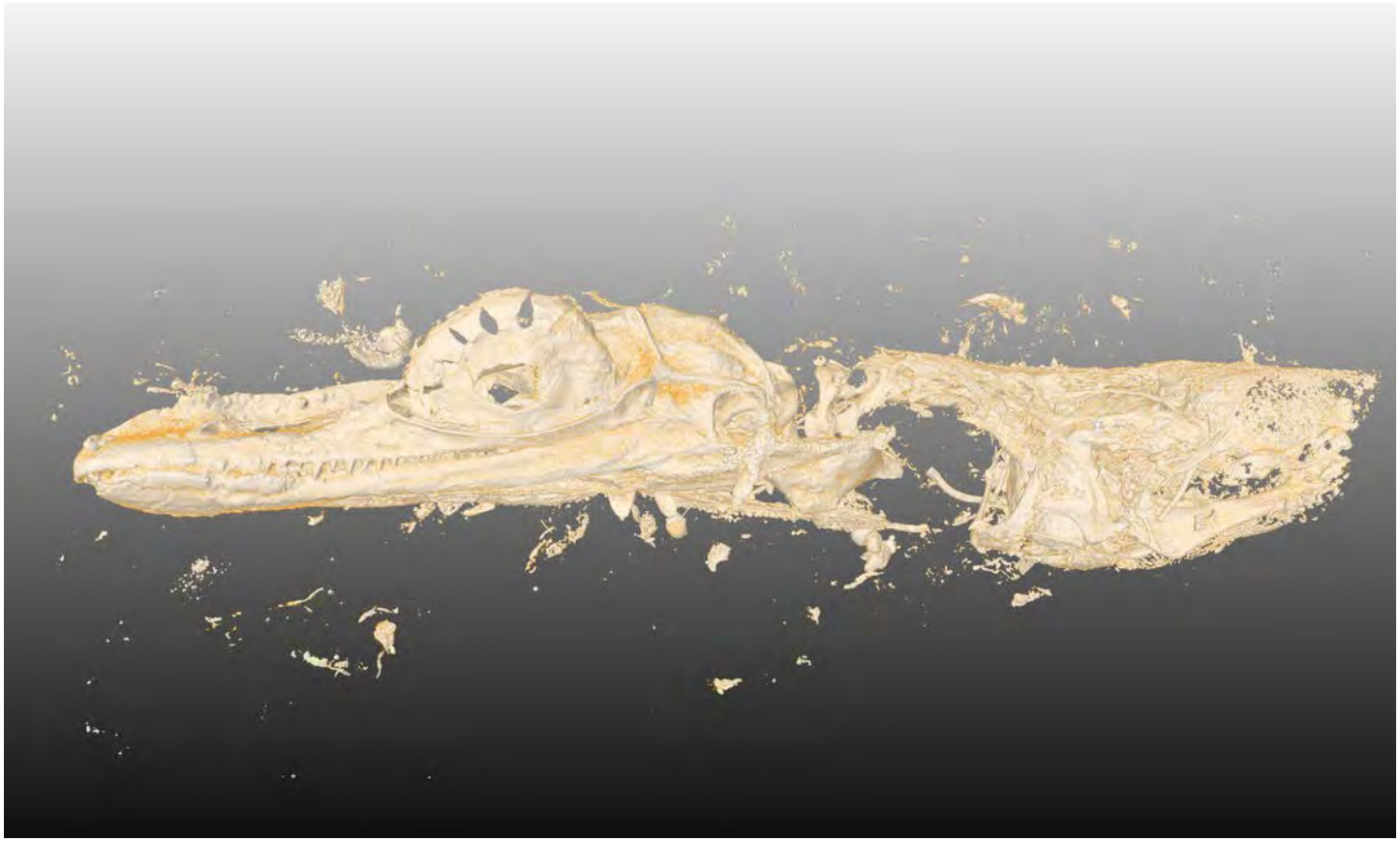

Fig. 48:

Fig. 49:

Fig. 50:

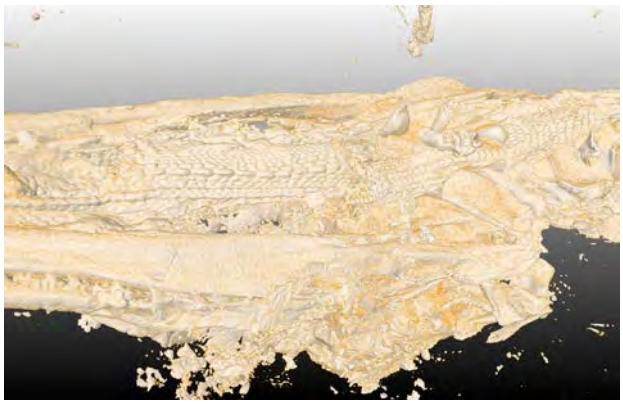

Fig. 51:

Fig. 52:

APPENDIX 5: SYNCHROTRON SCANNING OF GRS-REF-28627

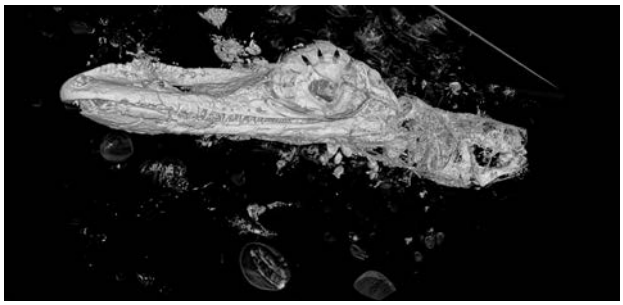

Fig. 53: Ref28627 snout

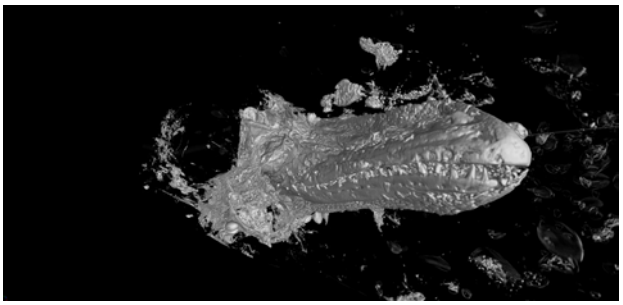

Fig. 54: Ref28627 snout detail

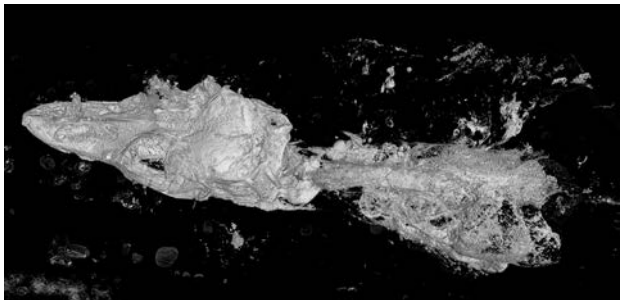

Fig. 55: Ref28627 head overview

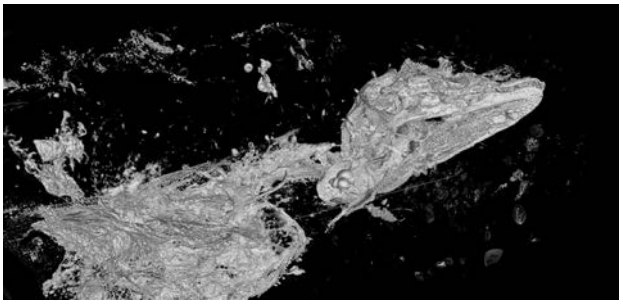

Fig. 56: Ref28627 overview underside

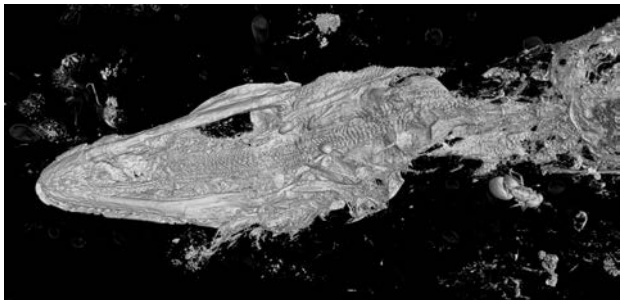

Fig. 57: Ref28627 lower jaw

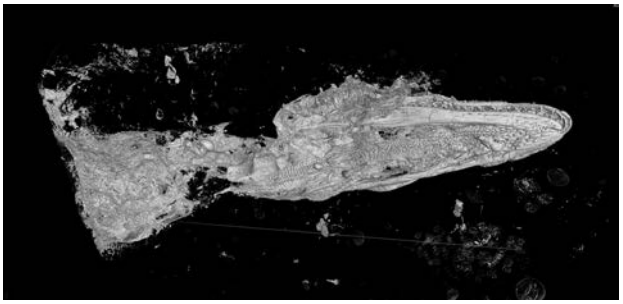

Fig. 58: Ref28627 lower jaw2

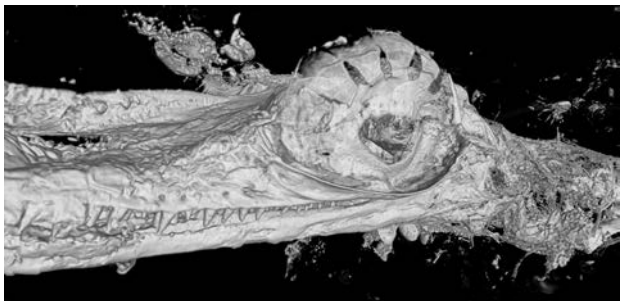

Fig. 59: Ref28627 eye

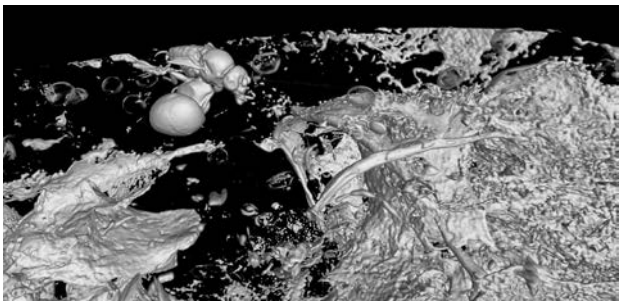

Fig. 60: Ref28627 fly

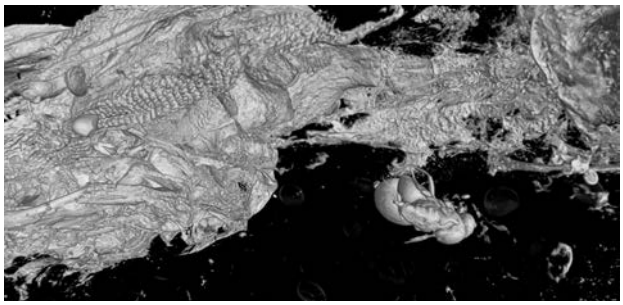

Fig. 61: Ref28627 insect01

Fig. 62: Ref28627 insect01 view2

APPENDIX 5: IMAGES OF GRS-REF-28627

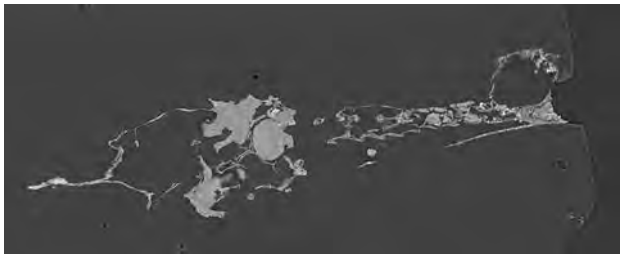

Fig. 63: Ref28627 braincase1

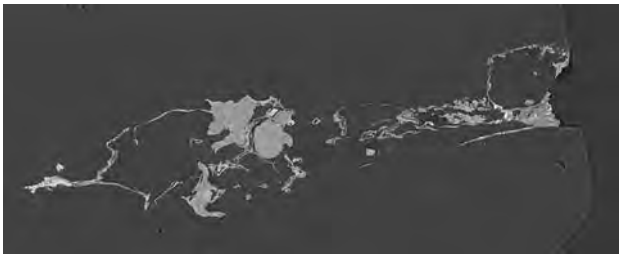

Fig. 64: Ref28627 braincase2

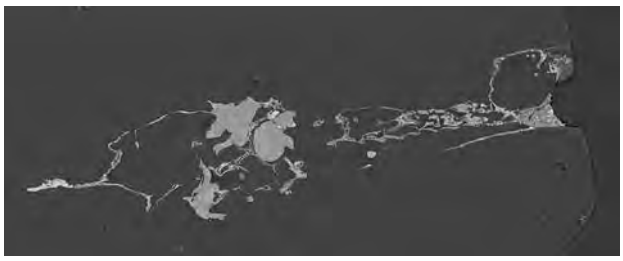

Fig. 65: Ref28627 braincase3

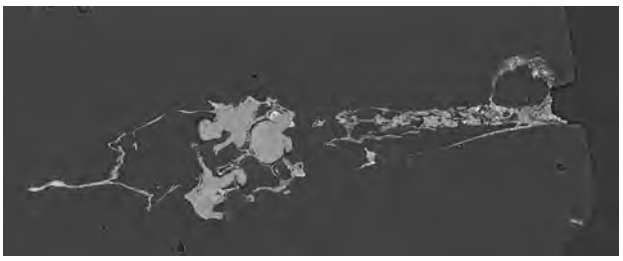

Fig. 66: Ref28627 spine

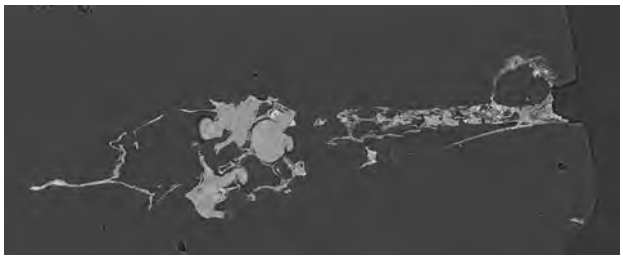

Fig. 67: Ref28627 spine2

Fig. 68: Ref28627 teeth internal

Fig. 69: Ref28627 teeth internal2

Fig. 70: Ref28627 teeth internal3

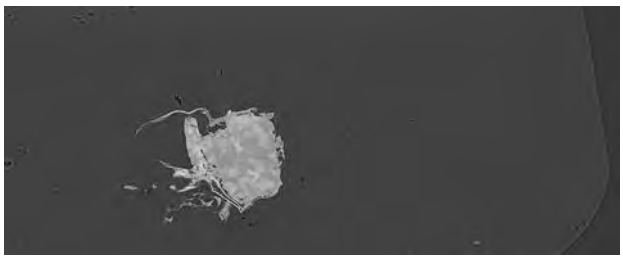

Fig. 71: Ref28627 hard palate

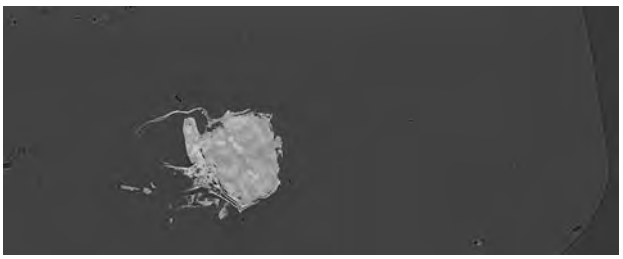

Fig. 72: Ref28627 hard palate2

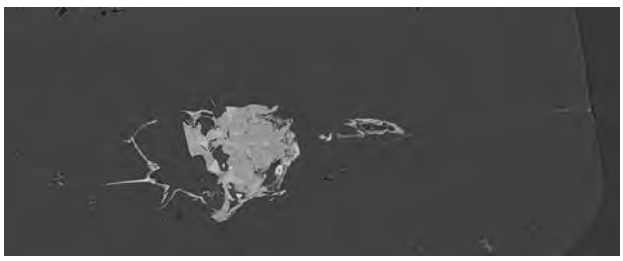

Fig. 73: Ref28627 brain and internal bone structure

APPENDIX 6: DATA COLLECTION OF GRS-REF-27746

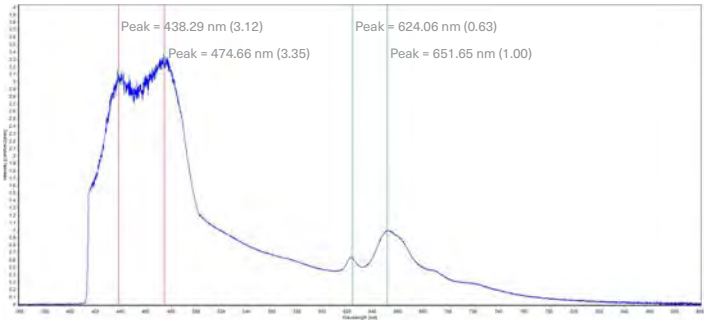

Fig. 74 GRS-Ref-27746_405_RT_200ms_20A_Sample_1

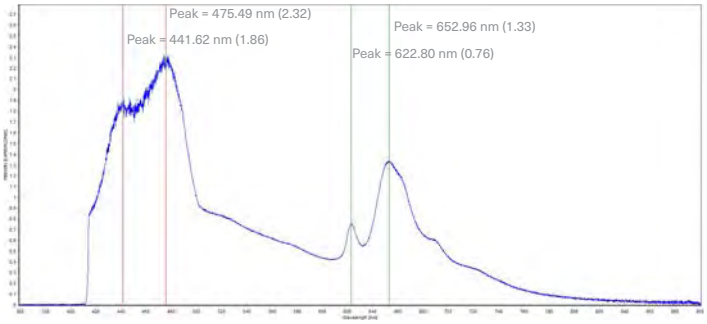

Fig. 75 GRS-Ref-27746_405_RT_200ms_20A_Sample_2

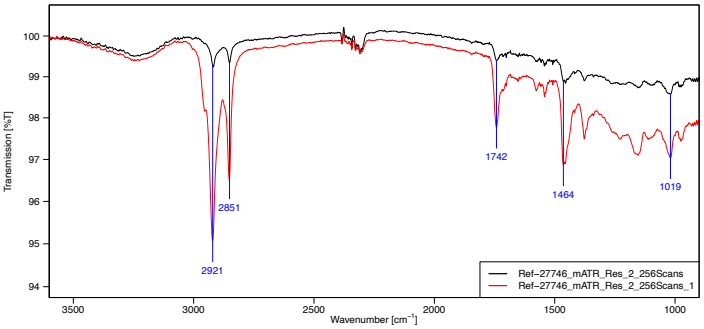

Fig. 76 GRS-Ref-27746-postcranial-skeleton_Res_4_256Scans

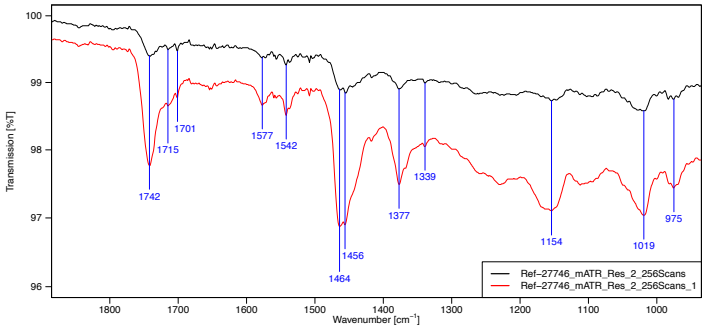

Fig. 77 GRS-Ref-27746-postcranial-skeleton_Res_4_256Scans_zoom

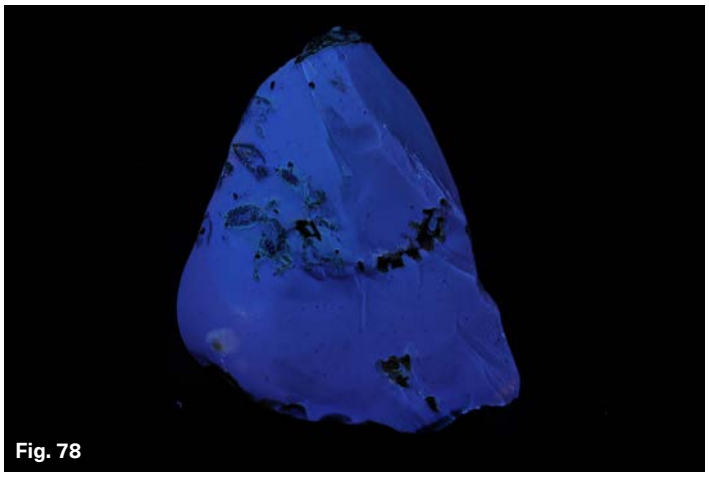

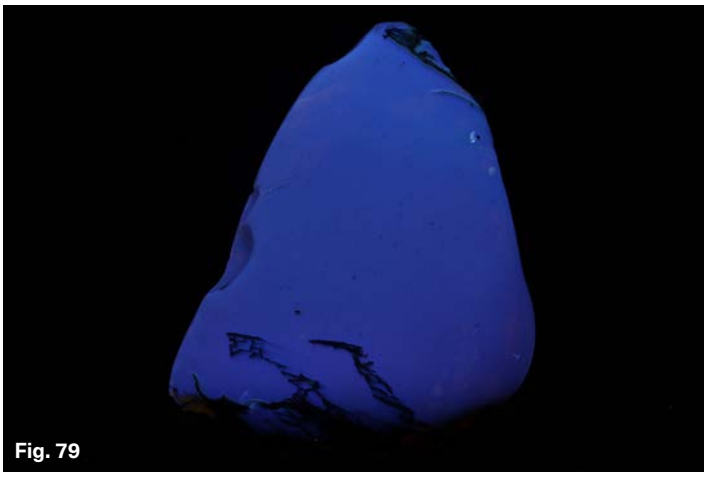

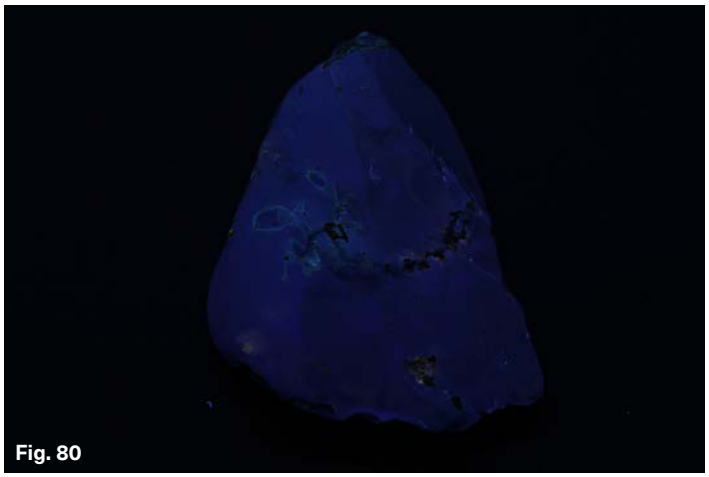

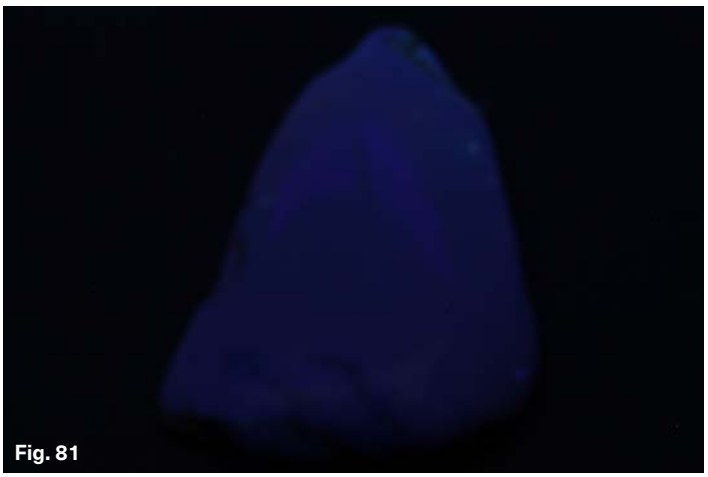

Fig. 78-81: Long-wave UV (365 nm), Fig. a) and b) and short-wave UV (254nm), Fig. c) and d) images of amber sample GRS-Ref-27746. The images were taken with a Canon EOS R camera using a 24-105 mm lens.

APPENDIX 7: INCLUSION IMAGES OF GRS-REF-27746

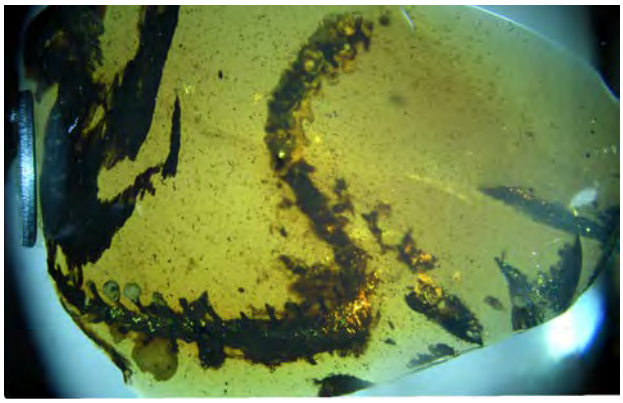

Fig. 82:

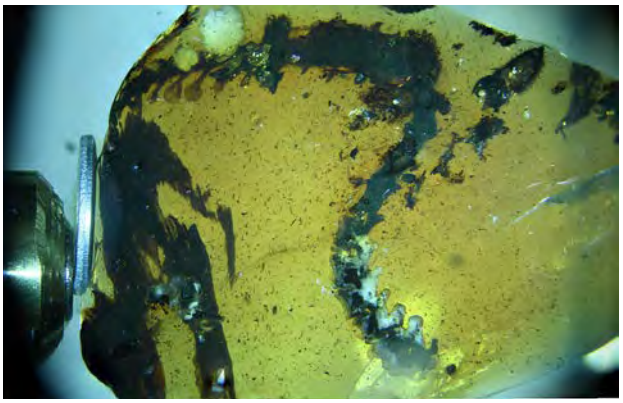

Fig. 83:

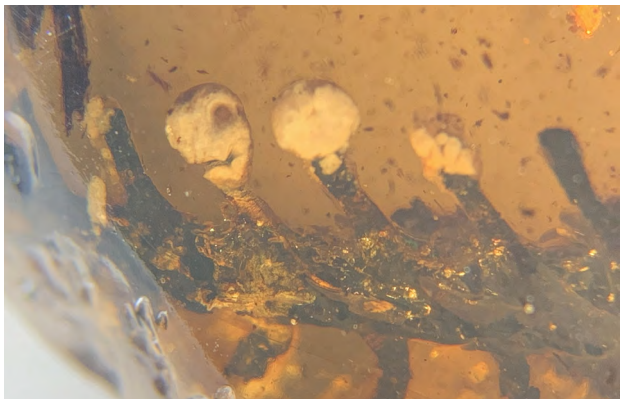

Fig. 84:

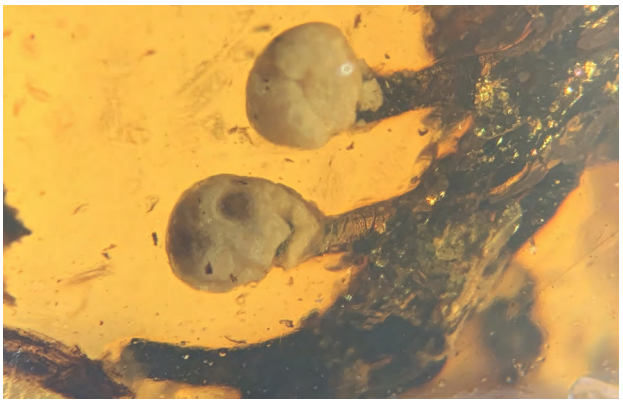

Fig. 85:

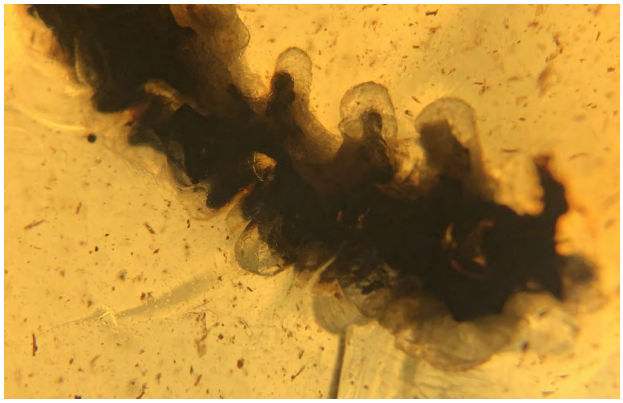

Fig. 86:

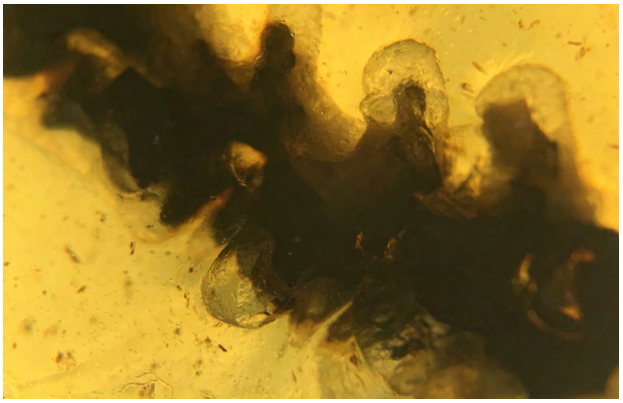

Fig. 87:

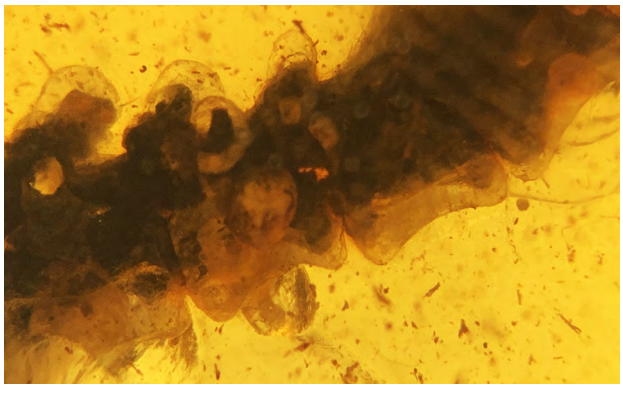

Fig. 88:

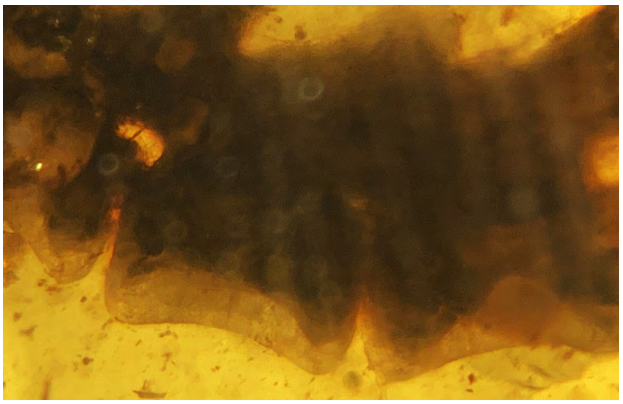

Fig. 89:

APPENDIX 8: IDENTIFICATION OF INSECT INCLUSIONS GRS-REF-27746

The following insects have been identified as a preliminary effort. The exact taxonomic identification is currently in progress and will be updated as soon as it is available.

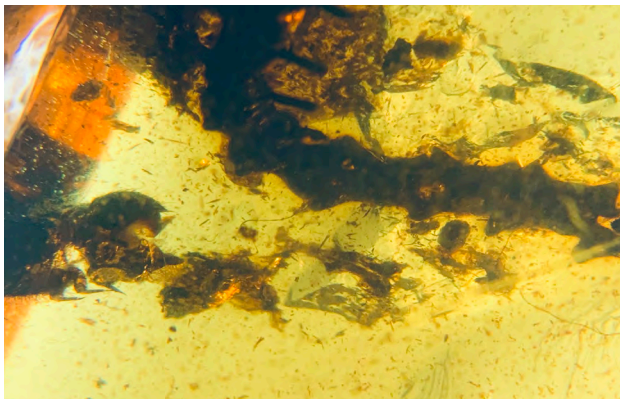

Fig. 90:

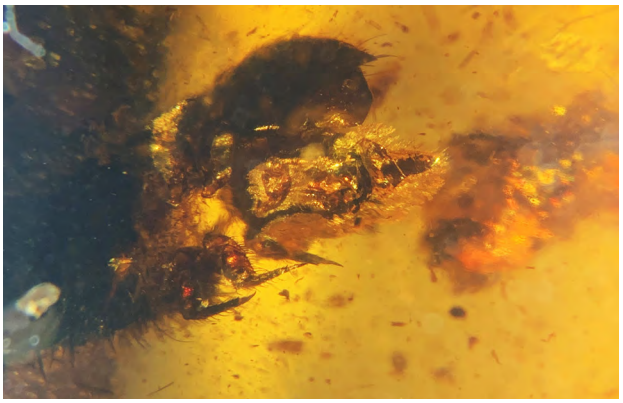

Fig. 91:

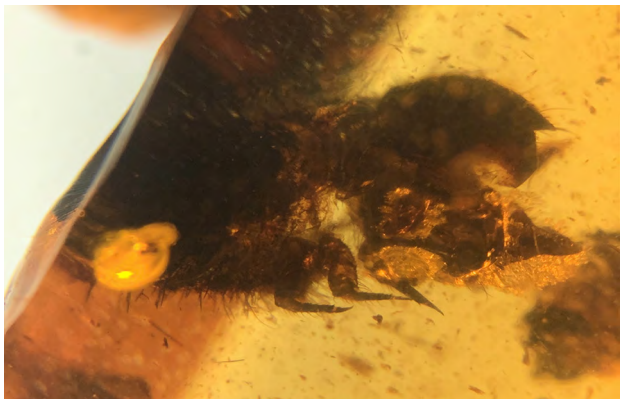

Fig. 92:

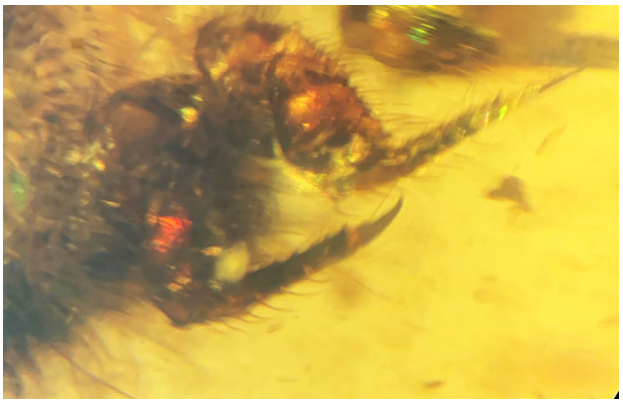

Fig. 93:

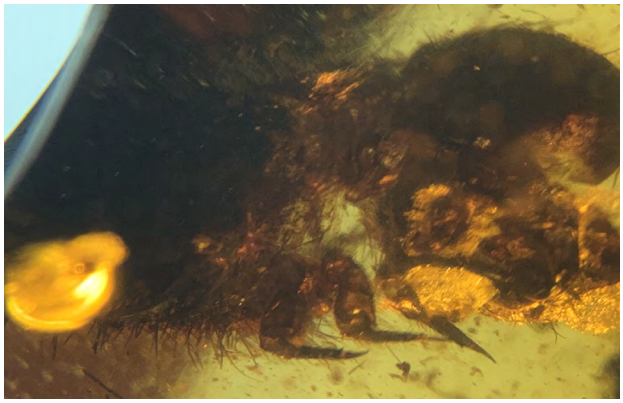

Fig. 94:

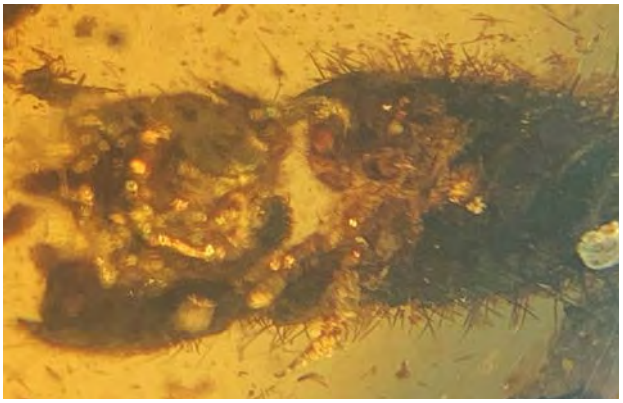

Fig. 95:

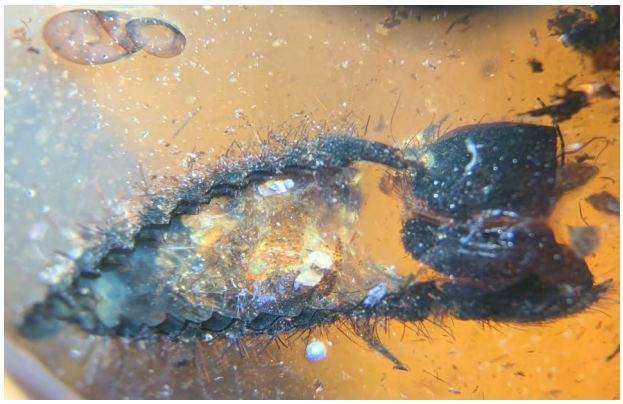

Fig. 96:

Fig. 97:

APPENDIX 8: INCLUSIONS GRS-REF-27746

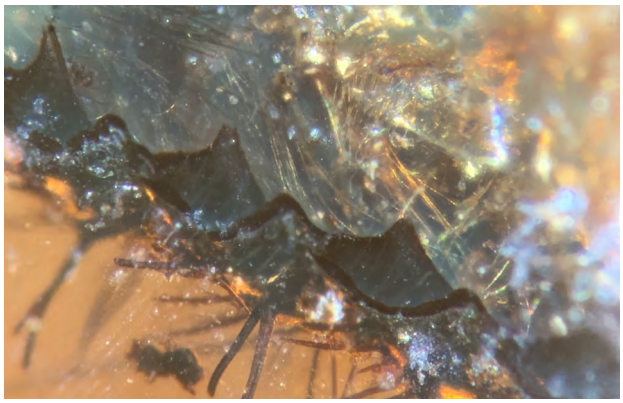

Fig. 98:

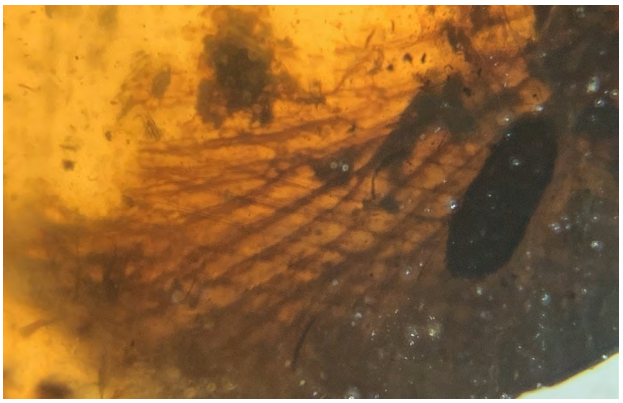

Fig. 99:

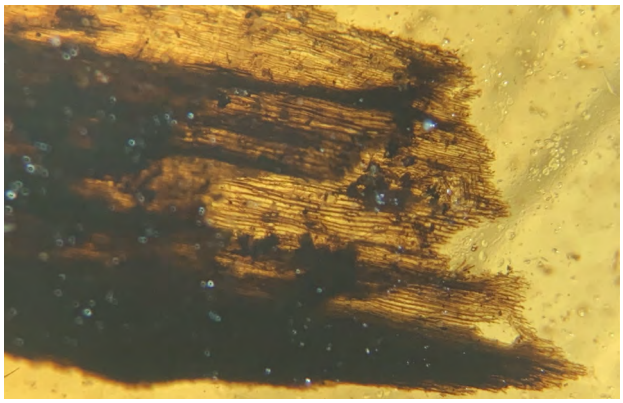

Fig. 100:

Fig. 101:

Fig. 102:

APPENDIX 9: CT SCANNING OF GRS-REF-27746

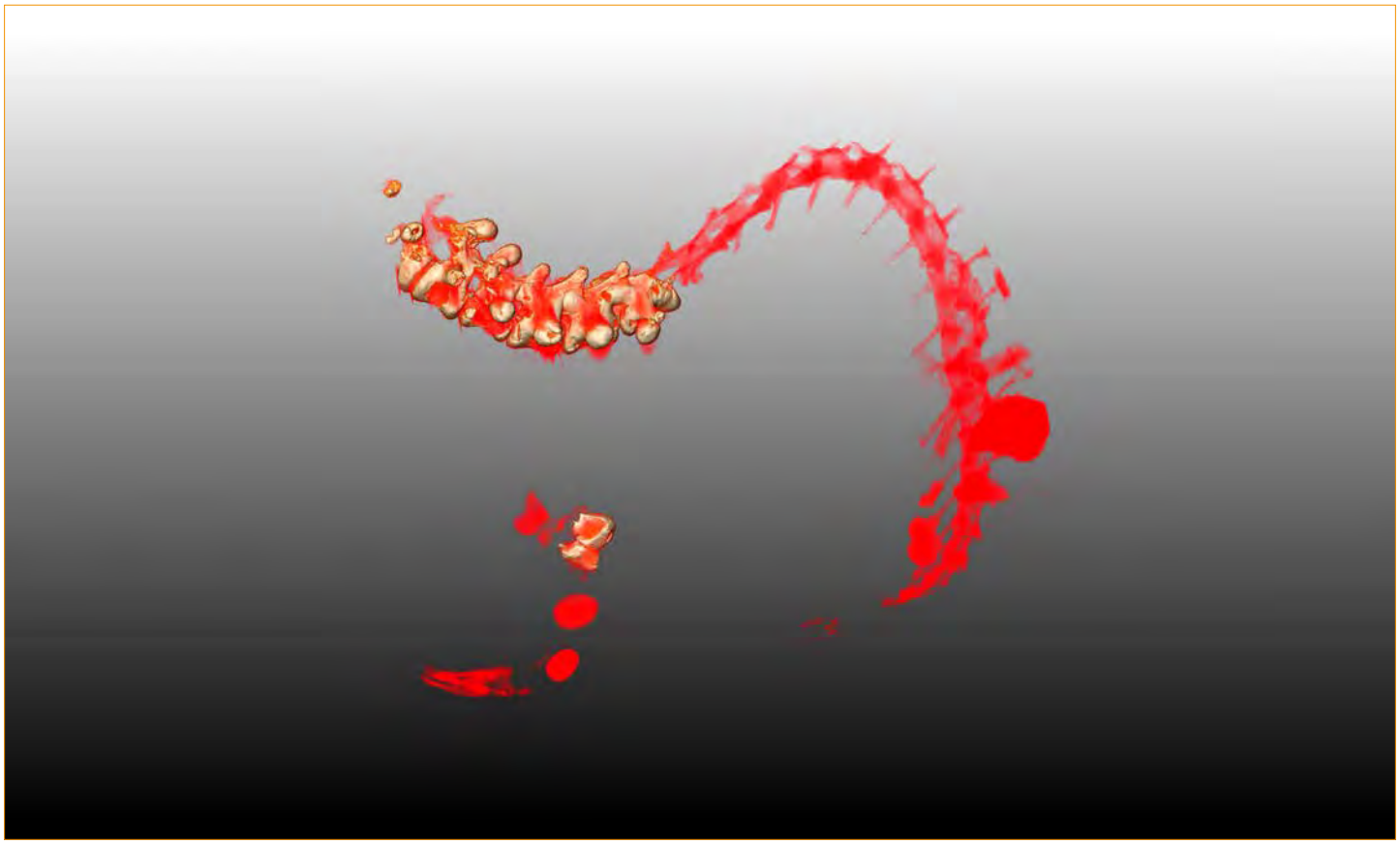

Fig. 103:

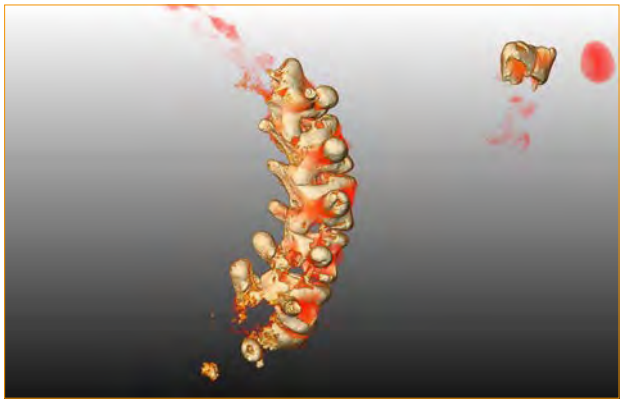

Fig. 104:

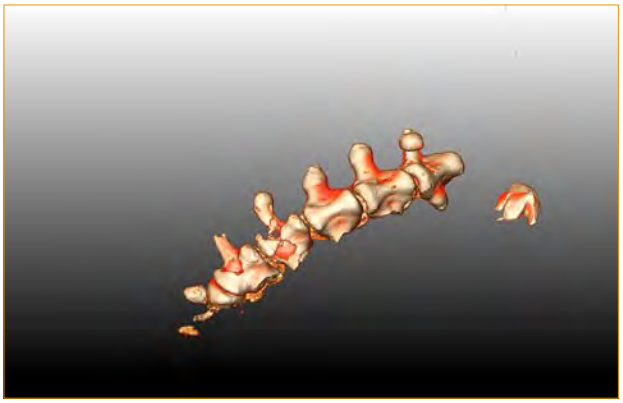

Fig. 105:

Fig. 106:

Fig. 107:

APPENDIX 10: DATA COLLECTION OF GRS-SREF-060829 YAKSHA PERETTII

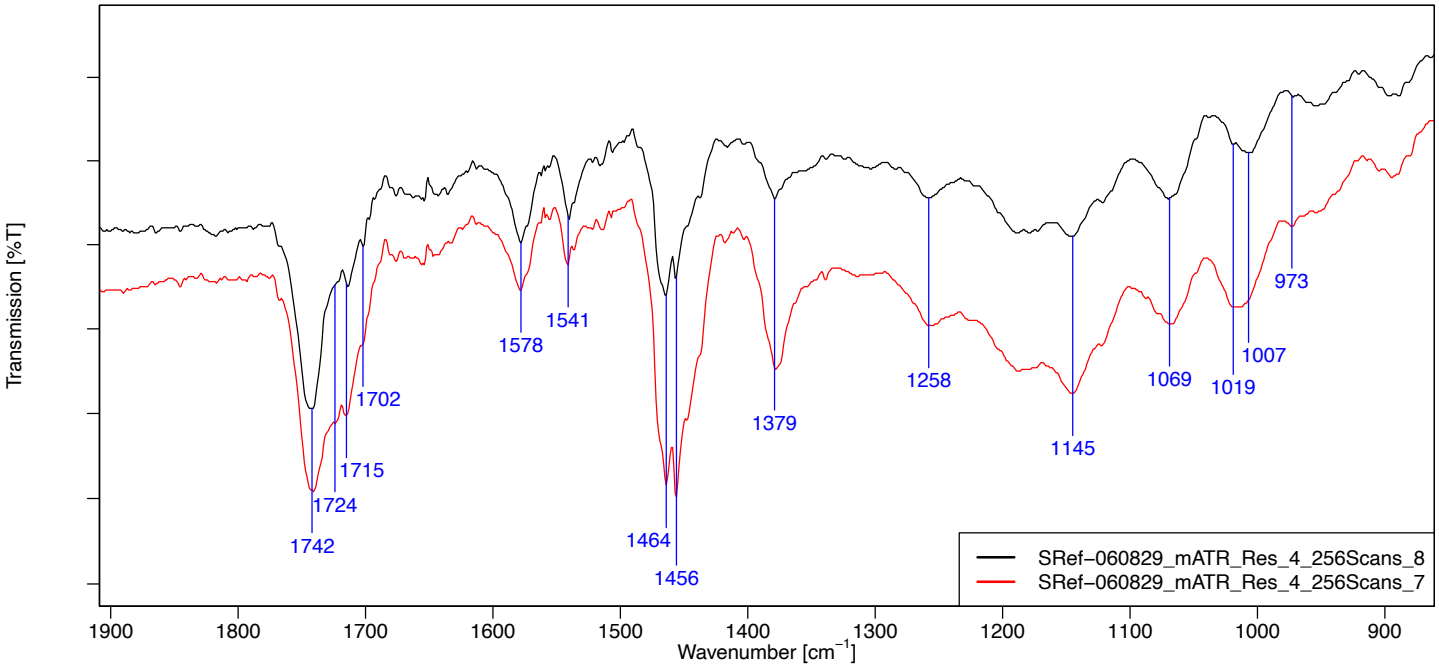

Fig. 108 GRS-SRef_060829_YakshaPerettii_mATR_Res_4_256Scans_zoom

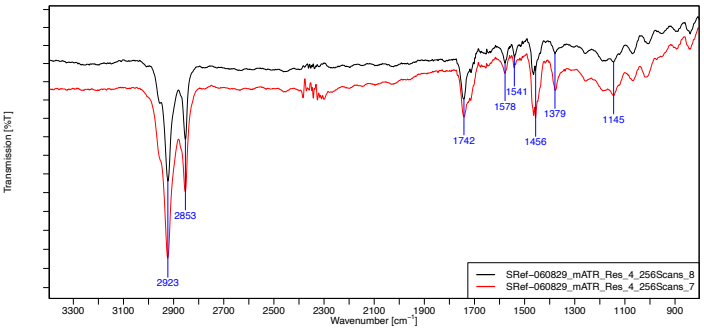

Fig. 109 GRS-SRef_060829_YakshaPerettii_mATR_Res_4_256Scans

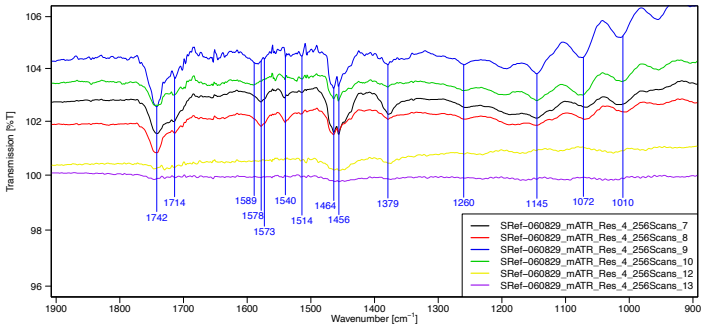

Fig. 110 mATR spectra of GRS-SRef-060829 Yaksha Perettii from multiple measuring points.

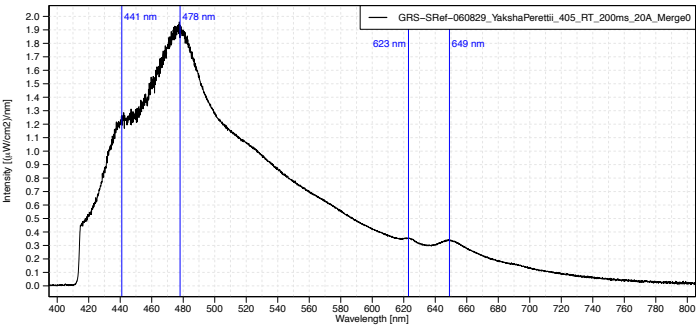

Fig. 111 GRS-SRef-060829_YakshaPerettii_405_RT_200ms_20A_2

APPENDIX 11: FLUORESCENCE IMAGES

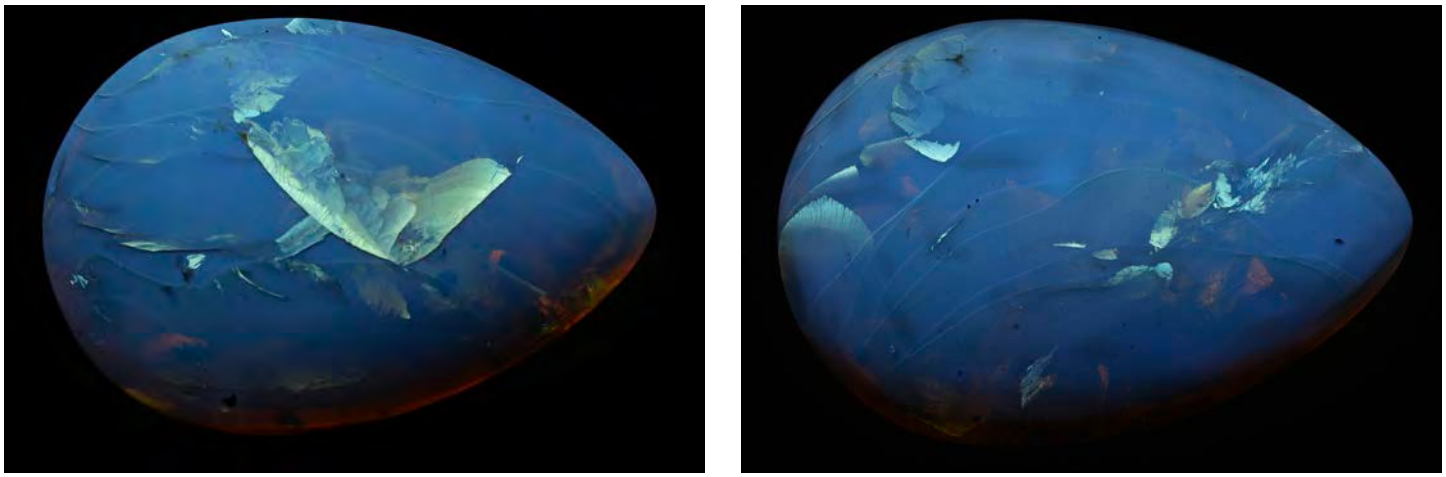

Fig. 112 Long-wave UV (365 nm) images of amber sample GRS-SRef-060829 Yaksha perettii (4 sec, f/14, ISO 200). Frontside (left) and backside (right).

APPENDIX 12: PICTURES OF YAKSHA PERETTI IN GRS-SREF-060829

Fig. 113 Sref-060829 A:

APPENDIX 12: PICTURES OF OF YAKSHA PERETTI IN GRS-SREF-060829

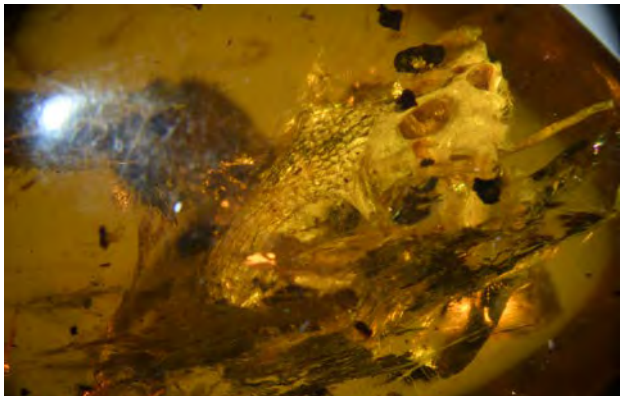

Fig. 114 Sref-060829 B:

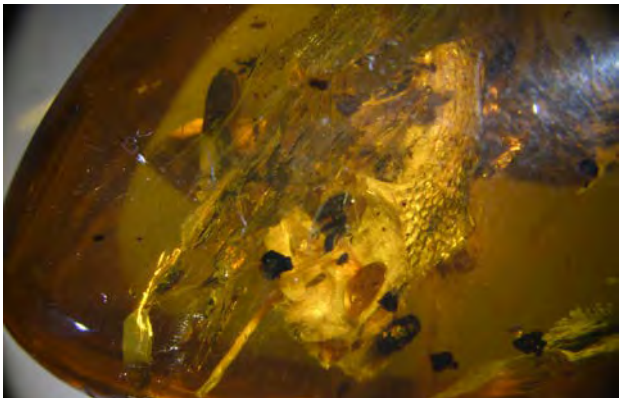

Fig. 115 Sref-060829 C :

Fig. 116 Sref-060829 D:

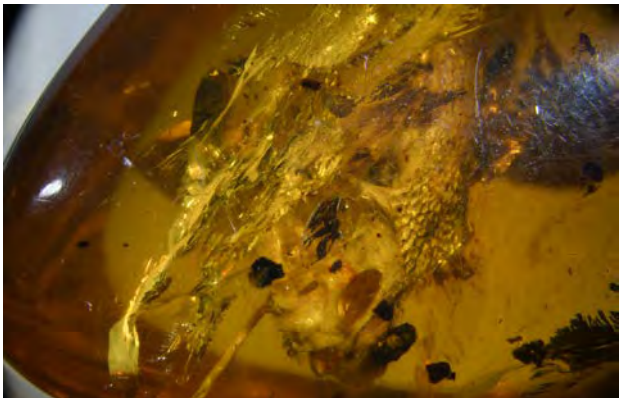

Fig. 117 Sref-060829 E:

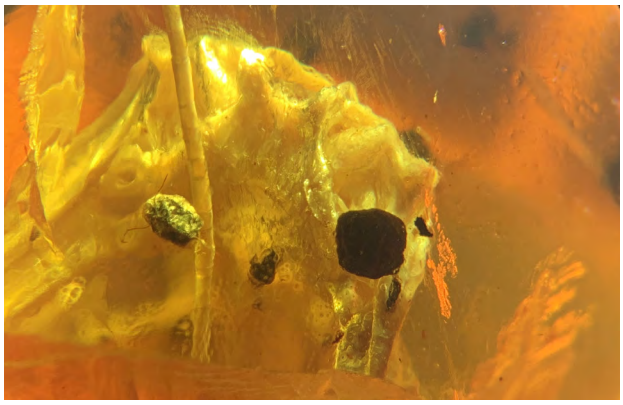

Fig. 118 Sref-060829 F:

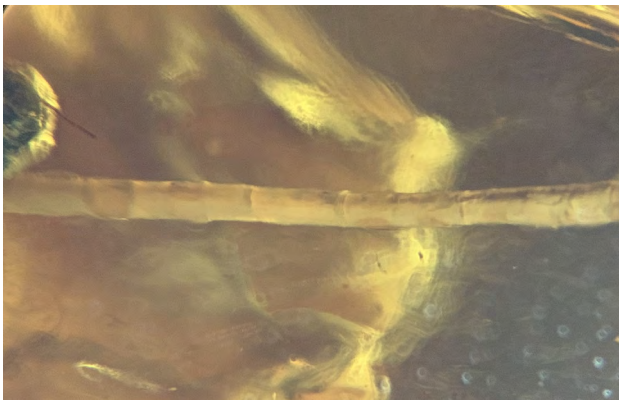

Fig. 119 Sref-060829 G:

APPENDIX 13: INSECT INCLUSIONS OF GRS-SREF-060829

The following insects have been identified as a preliminary effort. The exact taxonomic identification is currently in progress and will be updated as soon as it is available.

Fig. 120 Sref-060829 A:

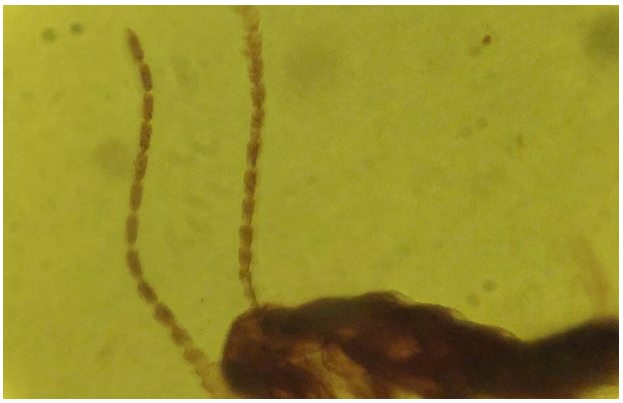

Fig. 121 Sref-060829 B:

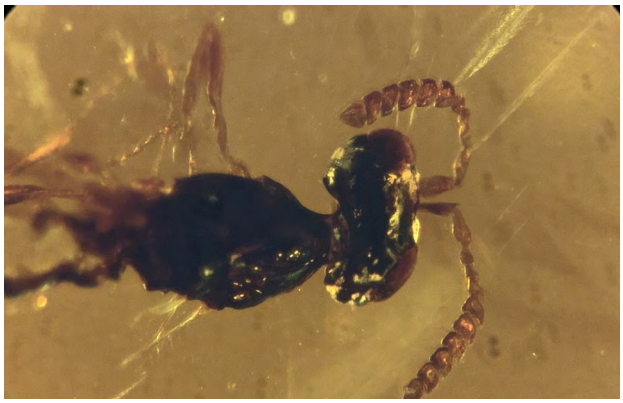

Fig. 123 Sref-060829 C :

Fig. 124 Sref-060829 D:

Fig. 125 Sref-060829 E:

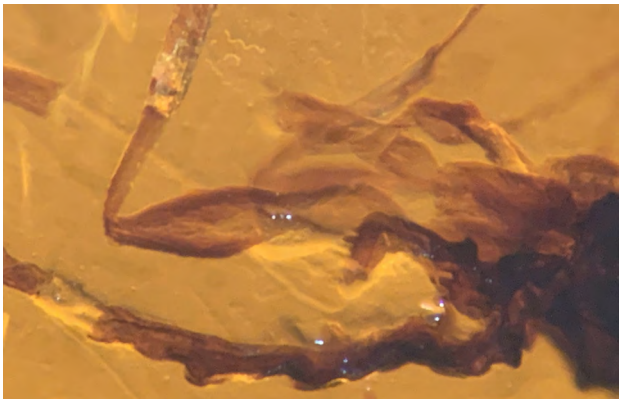

Fig. 126 Sref-060829 F:

Fig. 127 Sref-060829 G:

APPENDIX 14: PICTURES OF ORGANIC INCLUSION IN GRS-SREF-060829

Fig. 128 Sref-060829 A:

Fig. 128 Sref-060829 B:

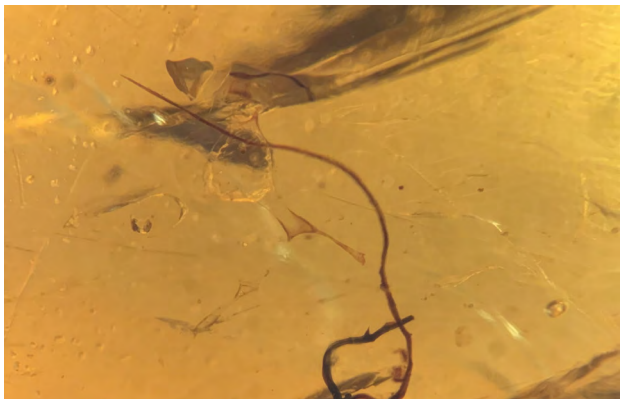

Fig. 129 Sref-060829 C :

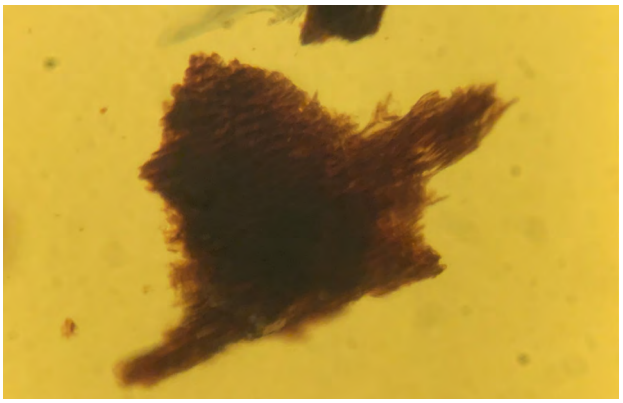

Fig. 130 Sref-060829 D:

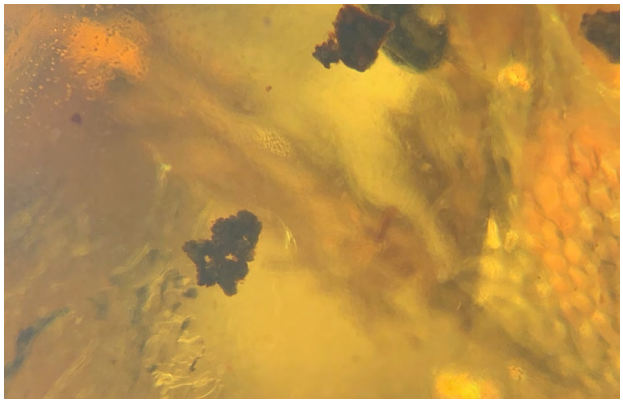

Fig. 131 Sref-060829 E:

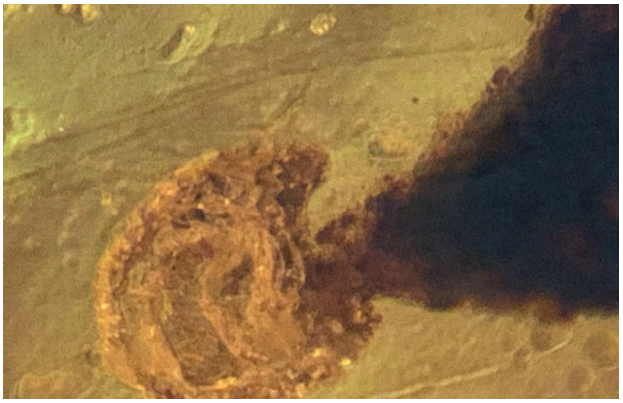

Fig. 132 Sref-060829 F:

APPENDIX 15: CT SCAN OF GRS-SREF-060829

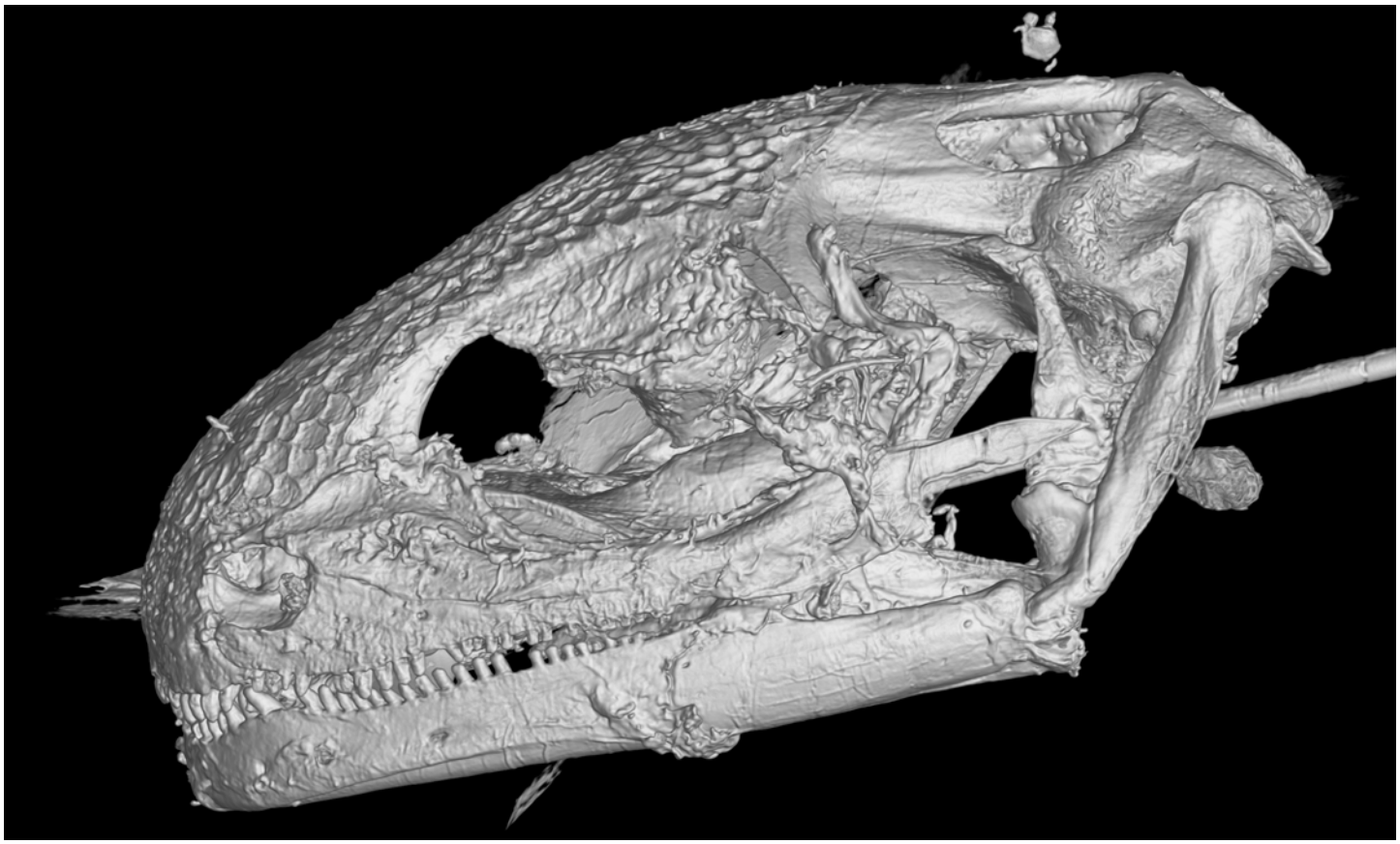

Fig. 133: SRef060829_Albi_side

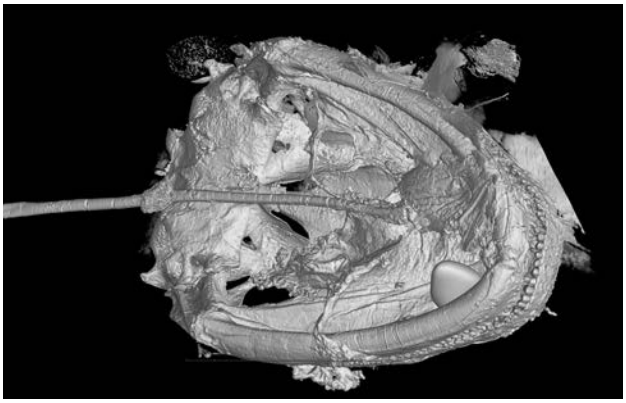

Fig. 134: SRef060829_Albi_angle2

Fig. 135: SRef060829_Albi_angle

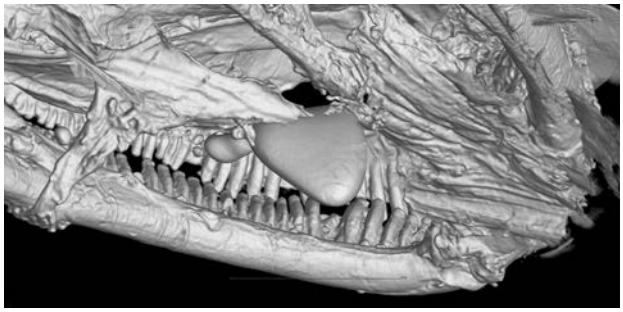

Fig. 136: SRef060829_Albi_internal

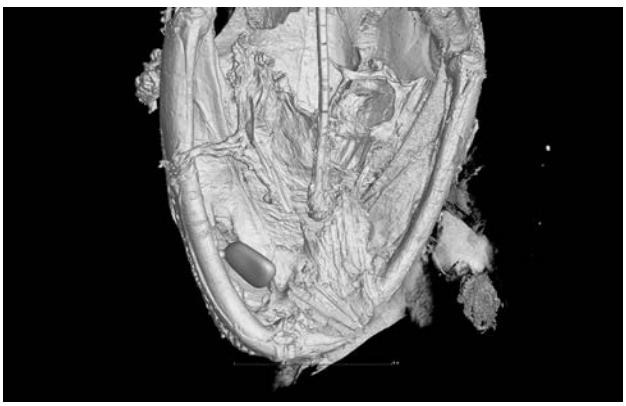

Fig. 137: SRef060829_Albi_toungue

APPENDIX 16: CT SCANNING OF GRS-SREF-060829

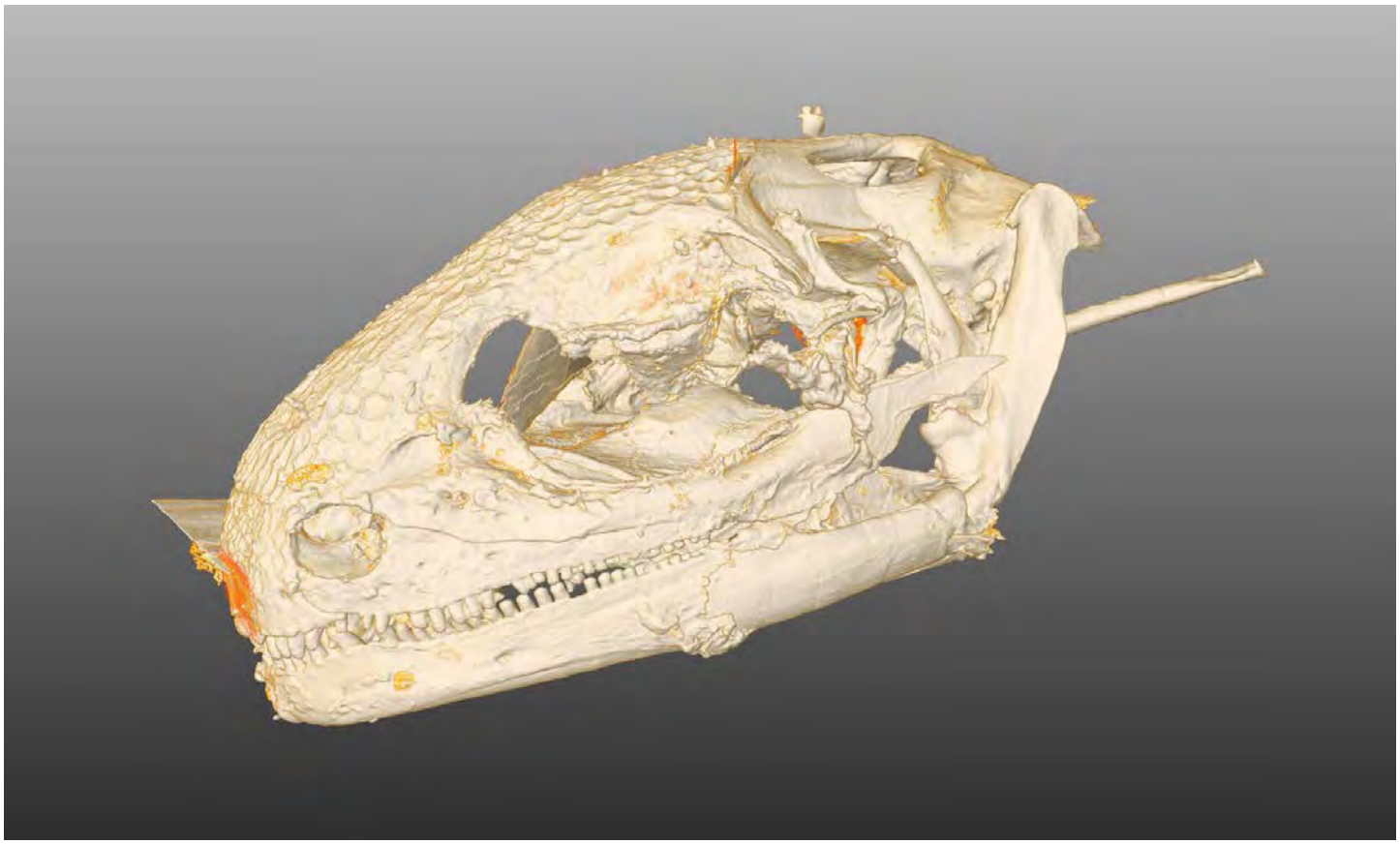

Fig. 138: Sref-060829-1 gr

Fig. 139: Sref-060829-2 wh

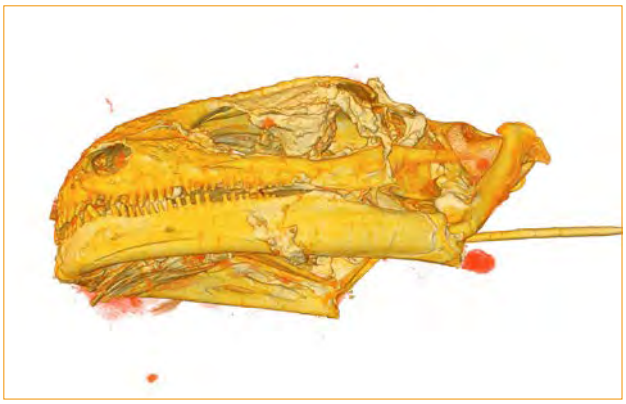

Fig. 140: Sref-060829-1

Fig. 141: Sref-060829-2

APPENDIX 17: PHOTOLUMINESCENCE TYPES

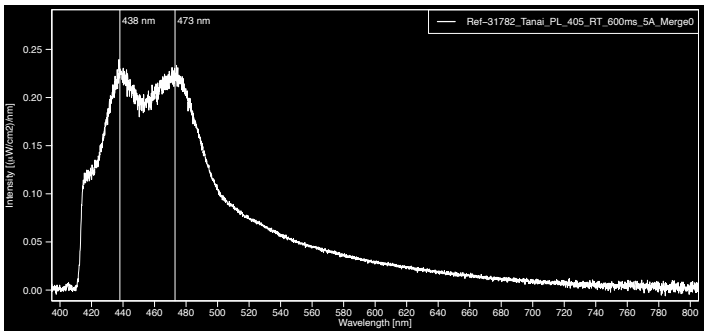

Fig. 142 Type A: Ref-31782; two large bands at around 440 and 470nm, no additional bands between 600 and 700 nm

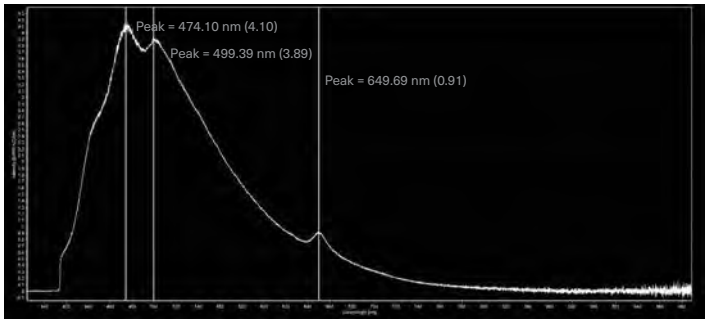

Fig. 143 Type B: Ref-30273; three bands at 440, 475 and 500 nm and additional band at 650nm

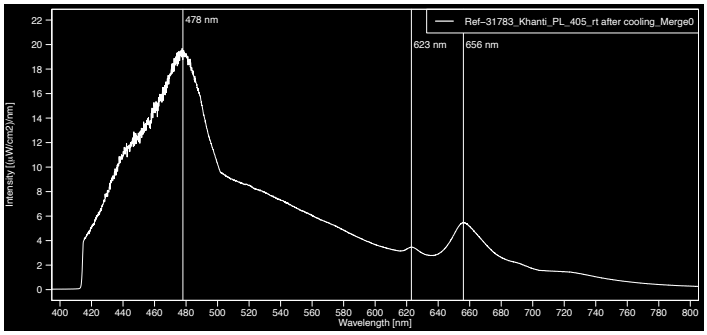

Fig. 144 Type C: Ref-31783; large band at 440 and 475 nm and additional small 2 lines at 625nm and 650nm

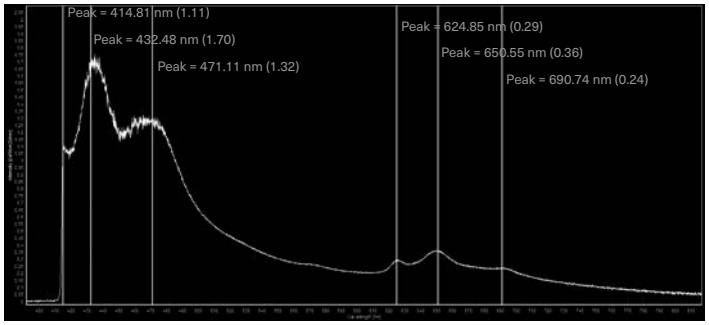

Fig. 145 Type D: Ref-31785; large band at 440 and 475, additional small 3 lines at 625, 650 and 690nm

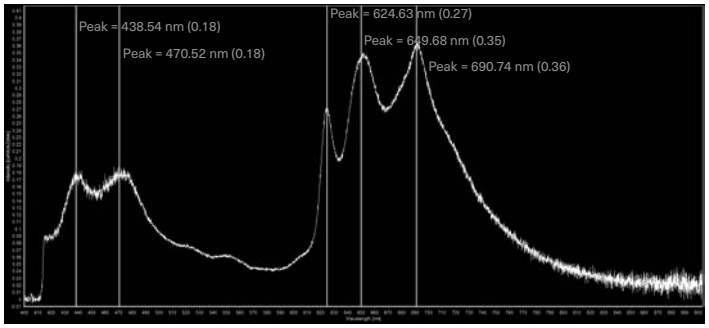

Fig. 146 Type E: GRS-Ref-27816; relative ratios between the bands is different, e.g. the bands in the red emission colors are more prominent

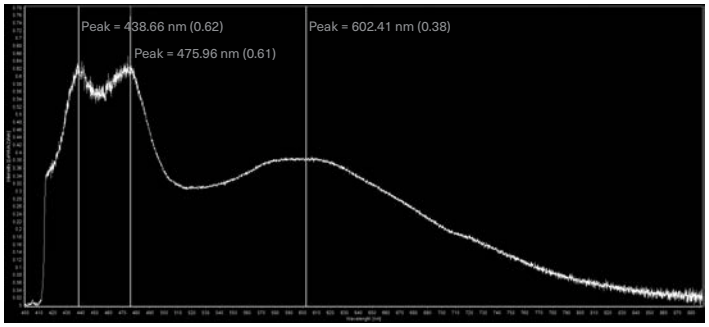

Fig. 147 Type F: GRS-Ref-31763a; large band at 440 and 475 nm and additional broad luminescence band around 600 nm

APPENDIX 17: PHOTOLUMINESCENCE TYPES

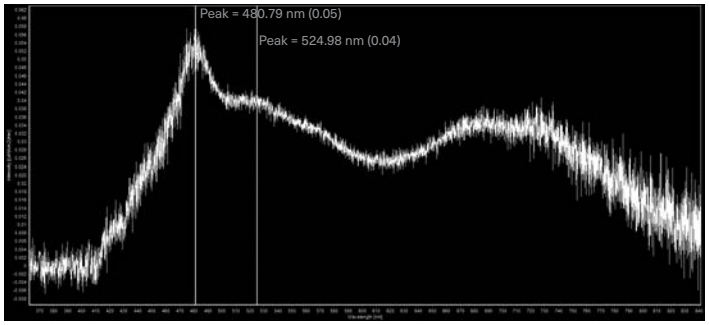

Fig. 148 Type G: GRS-Ref-31763a_; generally, very low PL intensity

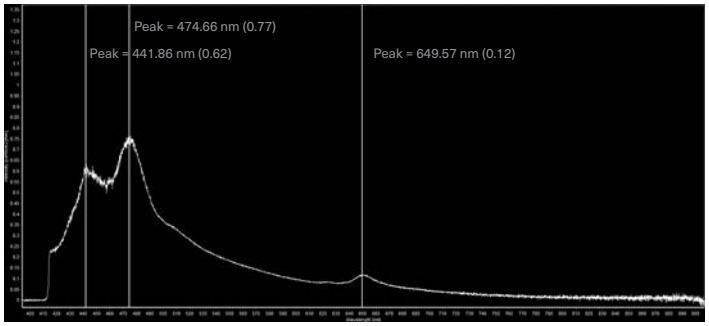

Fig. 149 GRS-Ref-31772

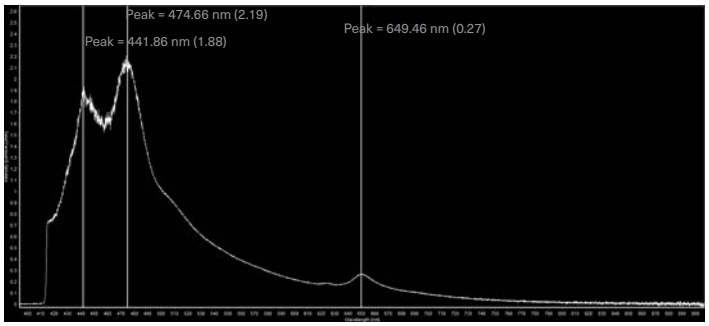

Fig. 150 GRS-Ref-31772

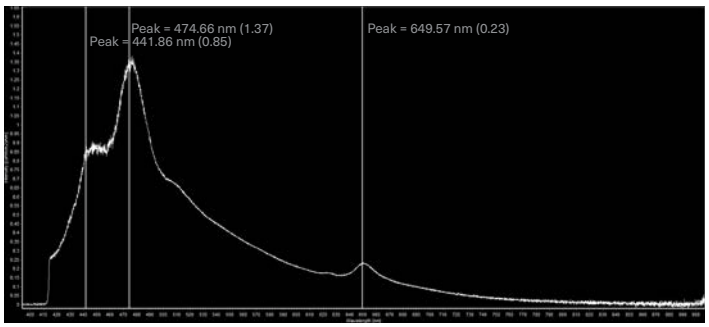

Fig. 151 GRS-Ref-31772

Number	Weight (ct)	Comment	Type A Two large bands at around 440 and 470nm, no additional bands between 600 and 700nm	Type B Three bands at 440, 475 and 500 nm and additional band at 650nm	Type C Large band at 440 and 470 nm and additional small 2 bands at 625nm and 650nm	Type D Large band at 440 and 475, additional small 3 bands at 625, 650 and 690nm	Type E Relative ratios between the bands is different, e.g. the bands in the red emission colors are more prominent	Type F Large band at around 440 and 470nm and additional broad luminescence band around 600nm	Type G Generally very low PL intensity
GRS-SRef-060829_ YakshaPerettii					Aungbar?				
GRS-Ref-28627_ Oculudentavis Naga	33.275		Aungbar?						
GRS-Ref-31782_ Aungbar_Tanai			Aungbar, Tanai						
GRS-Ref-31785_ Aungbar_Tanai	63.473					Aungbar, Tanai			
GRS-Ref-31758_ Augbar_Tanai_ MaiKhun									Aungbar, Tanai, Mai Khun
GRS-Ref-30273_ Aungbar	21.909			Aungbar					
GRS-Ref-30933_ Aungbar	12.961								
GRS-Ref-30966_ Aungbar	23.202								
GRS-Ref-31764_ ZeePhyueKone	5.492		Zee Phyue Kone						
GRS-Ref-27816_ Khamti	5.748	Color-change					Khamti, New Mine		
GRS-Ref-31992_ Khamti	26.488	LW-UV: Pink					Khamti		
GRS-Ref-31991_ Khamti	79.333	LW-UV: Pink					Khamti		
GRS-Ref-31774_ Khamti	7.445				Khamti				
GRS-Ref-31793_ Khamti_KyatMaw	9.905		Khamti, KyatMaw						
GRS-Ref-31763a_ HtiLin								Hti Lin, Kyar Khé, Tiger Bite	
GRS-Ref-31763b_ HtiLin								Hti Lin, Kyar Khé, Tiger Bite	
GRS-Ref-31770_ Aungbar_Tanai_ YarMut			Aungbar, Tanai, Yar Mut						
GRS-Ref-31772_ Aungbar_Tanai_ YarMut_Sample 1			Aungbar, Tanai, Yar Mut						
GRS-Ref-31772_ Aungbar_Tanai_ YarMut_Sample 2					Aungbar, Tanai, Yar Mut				